Group 11 complexes with phosphanylphosphaalkene ligand: preparation and stability study

A. Ziółkowska,[a] *N. Szynkiewicz,*[a] *J. Ryl,*[b] *Ł. Ponikiewski**[a]

[a] Department of Inorganic Chemistry, Chemical Faculty, Gdansk University of Technology, 11/12 Gabriela Narutowicza Str., 80-233 Gdansk, Poland.

[b] Institute of Nanotechnology and Materials Engineering, Faculty of Applied Physics and Mathematics, Gdansk University of Technology, 11/12 Gabriela Narutowicza Str., 80-233 Gdansk, Poland.

KEYWORDS: organometallic chemistry, diphosphorus ligand, transition metal phosphides.

PART A. EXPERIMENTAL SECTION 3
PART B. X-RAY CRYSTALLOGRAPHIC DATA 10
PART C. NMR SPECTUM SECTION 15
1. Reactions of phosphanylphosphaalkenes with CuCl 15
1.1. Reaction of Ph_2C=P-P*t*Bu_2 with CuCl. 15
1.2. Reaction of (*p*-MeO-Ph)$_2$C=P-P*t*Bu_2 with CuCl. 19
2. Reactions of phosphanylphosphaalkenes with AgCl 23
2.1 Reaction of Ph_2C=P-P*t*Bu_2 with AgCl. 23
2.2. Reaction of (*p*-MeO-Ph)$_2$C=P-P*t*Bu_2 with AgCl. 26
3. Reaction of phosphanylphosphaalkenes with (tht)AuCl. 30
3.1 Reaction of Ph_2C=P-P*t*Bu_2 with (tht)AuCl. 30
3.2. Reaction of (*p*-MeO-Ph)$_2$C=P-P*t*Bu_2 with (tht)AuCl. 34
PART D. DFT RESULTS 38
PART E. EDS analysis 47
PART F. REFERENCES 50

PART A. EXPERIMENTAL SECTION

1. General information

All synthetic reactions were conducted under an argon atmosphere using a standard Schlenk technique. Toluene and THF were dried over Na/benzophenone and were freshly distilled under argon prior to use. ^{1}H, ^{31}P and ^{13}C NMR spectra in solution were recorded on a Bruker AV400 MHz (external standard: tetramethylsilane for ^{1}H and ^{13}C, 85% H_3PO_4 for ^{31}P). The phosphanylphosphaalkenes used were synthesized according to the literature.[28] CuCl, AgCl and (tht)AuCl were purchased commercially.

2. Syntheses of the complexes.

2.1. Reactions of Ph_2C=P-P*t*Bu_2 or (*p*-MeO-Ph)$_2$C=P-P*t*Bu_2 with CuCl.

2.1.1. Synthesis of [Ph_2C=P-P(*t*Bu_2)-CuCl]$_2$ (Cu1).

Ph_2C=P-P*t*Bu_2 (100 mg, 0.292 mmol) was weighed together with CuCl (29 mg, 0.292 mmol) in a Schlenk tube and then 8 mL of THF was added. The initially orange solution was mixed for 48 hours. After this time, the solution color changed from orange to orange–brown, and a precipitate was observed. The solution was evaporated under vacuum, and then 60 mL of toluene was added. After filtration, the clear dark orange solution was concentrated to a 10 mL volume and stored at +4°C. After two days, orange crystals characterized as **Cu1** appeared (181 mg, yield 70%). Calculated elemental analysis (%) for $C_{42}H_{56}Cl_2P_4Cu_2$: C, 57.14; H, 6.39. Found: C, 57.05; H, 6.47; melting point: 256-257°C.

^{1}H NMR (400 MHz, $CDCl_3$, 298 K) δ 7.59, 7.51, 7.45, 7.32, 7.21 (20H, [**Ph**$_2$C=P-P(*t*Bu_2)-CuCl]$_2$ – H_{Ar}), 1.44 (d, $J_{P\text{-}H}$ = 14.1 Hz, 36 H, [Ph_2C=P-P(***t*Bu**$_2$)-CuCl]$_2$) ppm.

$^{13}C\{^{1}H\}$ NMR (100.6 MHz, $CDCl_3$, 298 K) δ 209.3 (d, $J_{P\text{-}C}$ = 60.2 Hz, [Ph_2**C**=P-P(*t*Bu_2)-CuCl]$_2$ – very weak signal located according to the $^{13}C\{^{1}H\}/^{1}H$-HMBC NMR spectrum), 145.46 (dd, $J_{P\text{-}C}$ = 25.9 Hz, $J_{P\text{-}H}$ = 8.1 Hz, [**Ph**$_2$C=P-P(*t*Bu_2)-CuCl]$_2$ – C_{Ar}), 144.63 (dd, $J_{P\text{-}C}$ = 13.6 Hz, $J_{P\text{-}H}$ = 9.7 Hz, [**Ph**$_2$C=P-P(*t*Bu_2)-CuCl]$_2$ – C_{Ar}), 130.76 (d, $J_{P\text{-}C}$ = 5.0 Hz, [**Ph**$_2$C=P-P(*t*Bu_2)-CuCl]$_2$ – C_{Ar}),

130.13 (s, $J_{P\text{-}C}$ = 5.0 Hz, [**Ph**$_2$C=P-P(tBu$_2$)-CuCl]$_2$ – C_{Ar}), 128.42 (d, $J_{P\text{-}C}$ = 0.9 Hz, [**Ph**$_2$C=P-P(tBu$_2$)-CuCl]$_2$ – C_{Ar}), 127.39 (d, $J_{P\text{-}C}$ = 20.0 Hz, [**Ph**$_2$C=P-P(tBu$_2$)-CuCl]$_2$ – C_{Ar}), 127.02 (dd, $J_{P\text{-}C}$ = 6.4 Hz, $J_{P\text{-}H}$ = 1.8 Hz, [**Ph**$_2$C=P-P(tBu$_2$)-CuCl]$_2$ – C_{Ar}), 36.44 (dd, $J_{P\text{-}C}$ = 8.0 Hz, $J_{P\text{-}H}$ = 5.5 Hz, [Ph$_2$C=P-P{**C**(CH$_3$)$_2$}-CuCl]$_2$), 30.93 (dd, $J_{P\text{-}C}$ = 6.44 Hz, $J_{P\text{-}H}$ = 1.8 Hz, [Ph$_2$C=P-P{C(**C**H$_3$)$_2$}-CuCl]$_2$) ppm.

^{31}P{^{1}H} NMR (162 MHz, $CDCl_3$, 298 K) δ 231.17 (d, $J_{P\text{-}P}$ = 268.7 Hz, [Ph$_2$C=**P**-P(tBu$_2$)-CuCl]$_2$), 37.44 (d, $J_{P\text{-}P}$ = 268.7 Hz, [Ph$_2$C=P-**P**(tBu$_2$)-CuCl]$_2$) ppm.

2.1.2. Synthesis of [(p-MeO-Ph)$_2$C=P-P(tBu$_2$)-CuCl]$_2$ (Cu2).

(p-MeO-Ph)$_2$C=P-PtBu$_2$ (100 mg, 0.248 mmol) was weighed together with CuCl (25 mg, 0.248 mmol) in a Schlenk tube, and then 10 mL of THF was added. The reaction solution was mixed for 24 hours. After this time, the initially red–orange solution color changed to brown–yellow. Additionally, the precipitate in the solution was observed. The solution was evaporated under vacuum, and then 15 mL of toluene was added. After filtration, the clear orange solution was concentrated to 5 mL and stored at +4°C. After two days, orange crystals characterized as **Cu2** appeared (212 mg, yield 72%). Calculated elemental analysis (%) for $C_{60}H_{80}Cl_2O_4P_4Cu_2$ (complex **Cu2** crystallized with one molecule of toluene in the unit cell): C, 60.70; H, 6.79. Found: C, 60.55; H, 6.85; melting point: 199-200°C.

^{1}H NMR (400 MHz, $CDCl_3$, 298 K) δ 7.33, 7.01, 6.74 ppm, 16H, [(p-MeO-**Ph**)$_2$C=P-P(tBu$_2$)-CuCl]$_2$ – H_{Ar}, from 7.20 to 7.05 (aromatic protons of one molecule of toluene), 3.86 (s, 3H, [(p-**M**eO-Ph)$_2$C=P-P(tBu$_2$)-CuCl]$_2$), 3.73 (s, 3H, [(p-**M**eO-Ph)$_2$C=P-P(tBu$_2$)-CuCl]$_2$)], 2.26 (s, methyl group protons of one molecule of toluene), 1.31 (d, $J_{P\text{-}H}$ = 14.2 Hz, 36 H, [(p-MeO-Ph)$_2$C=P-P(***t*Bu**$_2$)-CuCl]$_2$) ppm.

^{13}C{^{1}H} NMR (100.6 MHz, $CDCl_3$, 298 K) δ 208.32 (d, $J_{P\text{-}C}$ = 57.2 Hz, [(p-MeO-Ph)$_2$**C**=P-P(tBu$_2$)-CuCl]$_2$), 162.40 (d, $J_{P\text{-}C}$ = 4.4 Hz, [(p-MeO-**Ph**)$_2$C=P-P(tBu$_2$)-CuCl]$_2$ – C_{Ar}), 160.72 (s,

[(*p*-MeO-**Ph**)$_2$C=P-P(*t*Bu$_2$)-CuCl]$_2$ – C$_{Ar}$), 138.84 (dd, J_{P-C} = 26.8 Hz, J_{P-C} = 8.4 Hz, [(*p*-MeO-**Ph**)$_2$C=P-P(*t*Bu$_2$)-CuCl]$_2$ – C$_{Ar}$), 137.86 (s, toluene – C$_{Ar}$), 136.66 (dd, J_{P-C} = 13.5 Hz, J_{P-C} = 9.3 Hz, [(*p*-MeO-**Ph**)$_2$C=P-P(*t*Bu$_2$)-CuCl]$_2$ – C$_{Ar}$), 129.30 (d, J_{P-C} = 19.9 Hz, [(*p*-MeO-**Ph**)$_2$C=P-P(*t*Bu$_2$)-CuCl]$_2$ – C$_{Ar}$), 129.06 (s, [(*p*-MeO-**Ph**)$_2$C=P-P(*t*Bu$_2$)-CuCl]$_2$ – C$_{Ar}$), 128.76 (dd, toluene – C$_{Ar}$), 128.25 (s, toluene – C$_{Ar}$), 125.33 (s, toluene – C$_{Ar}$), 115.62 (s, [(*p*-MeO-**Ph**)$_2$C=P-P(*t*Bu$_2$)-CuCl]$_2$ – C$_{Ar}$), 113.80 (s, [(*p*-MeO-**Ph**)$_2$C=P-P(*t*Bu$_2$)-CuCl]$_2$ – C$_{Ar}$), 77.13 (t, chloroform), 36.35 (dd, J_{P-C} = 8.6 Hz, J_{P-C} = 5.4 Hz, [(*p*-MeO-Ph)$_2$C=P-P{**C**(CH$_3$)$_2$}-CuCl]$_2$), 31.05 (dd, J_{P-C} = 8.6 Hz, J_{P-C} = 5.4 Hz, [(*p*-MeO-Ph)$_2$C=P-P{C(**C**H$_3$)$_2$}-CuCl]$_2$) ppm.

^{31}P{^{1}H} NMR (162 MHz, CDCl$_3$, 298 K) δ 210.20 (d, J_{P-P} = 280.66 Hz, [(*p*-MeO-Ph)$_2$C=**P**-P(*t*Bu$_2$)-CuCl]$_2$), 40.82 (d, J_{P-P} = 280.66 Hz, [(*p*-MeO-Ph)$_2$C=P-**P**(*t*Bu$_2$)-CuCl]$_2$) ppm.

2.2. Reactions of Ph$_2$C=P-P*t*Bu$_2$ or (*p*-MeO-Ph)$_2$C=P-P*t*Bu$_2$ with AgCl.

2.2.1. Synthesis of [Ph$_2$C=P-P(*t*Bu$_2$)-AgCl]$_2$ (Ag1).

(Ph)$_2$C=P-P*t*Bu$_2$ (100 mg, 0.292 mmol) was weighed together with AgCl (42 mg, 0.292 mmol) in a Schlenk tube, and then 50 mL of THF was added. The reaction solution was mixed for 48 hours. After this time, the initially orange solution color changed to yellow. The solution was evaporated under vacuum, and then 40 mL of toluene was added. After filtration the clear yellow solution was concentrated to 10 mL and stored at +4°C. After 24 hours, yellow crystals characterized as **Ag1** appeared (184 mg, yield 65%). Calculated elemental analysis (%) for C$_{42}$H$_{56}$Cl$_2$P$_4$Ag$_2$: C, 51.93; H, 5.81. Found: C, 51.85; H, 5.89; melting point: 208-209°C.

^{1}H NMR (400 MHz, CDCl$_3$, 298 K) δ 7.62, 7.61, 7.48, 7.44, 7.34, 7.12, 7.10 (20H, [**Ph**$_2$C=P-P(*t*Bu$_2$)-AgCl]$_2$ – H$_{Ar}$), 1.42 (d, J_{P-H} = 14.8 Hz, [Ph$_2$C=P-P(***t*Bu$_2$**)-AgCl]$_2$) ppm.

^{13}C{^{1}H} NMR (100.6 MHz, CDCl$_3$, 298 K) δ 210.06 (dd, J_{P-C} = 57.2 Hz, J_{P-C} = 1.08 Hz, [Ph$_2$**C**=P-P(*t*Bu$_2$)-AgCl]$_2$), 144.91 (dd, J_{P-C} = 26.3 Hz, J_{P-H} = 8.2 Hz, [**Ph**$_2$C=P-P(*t*Bu$_2$)-AgCl]$_2$ – C$_{Ar}$), 142.84 (dd, J_{P-C} = 13.7 Hz, J_{P-H} = 10.2 Hz, [**Ph**$_2$C=P-P(*t*Bu$_2$)-AgCl]$_2$ – C$_{Ar}$), 131.20 (d, J_{P-C}

= 5.2 Hz, [**Ph**$_2$C=P-P(*t*Bu$_2$)-AgCl]$_2$ – C$_{Ar}$), 130.01 (s, [**Ph**$_2$C=P-P(*t*Bu$_2$)-AgCl]$_2$ – C$_{Ar}$), 128.57 (s, [**Ph**$_2$C=P-P(*t*Bu$_2$)-AgCl]$_2$ – C$_{Ar}$), 127.54 (d, J_{P-C} = 7.0 Hz, J_{P-C} = 1.6 Hz, [**Ph**$_2$C=P-P(*t*Bu$_2$)-AgCl]$_2$ – C$_{Ar}$), 127.12 (d, J_{P-C} = 20.4 Hz, [**Ph**$_2$C=P-P(*t*Bu$_2$)-AgCl]$_2$ – C$_{Ar}$), 36.43 (dd, J_{P-C} = 5.4 Hz, J_{P-H} = 4.3 Hz, [Ph$_2$C=P-P{**C**(CH$_3$)$_2$}-AgCl]$_2$), 30.93 (dd, J_{P-C} = 8.8 Hz, J_{P-H} = 4.6 Hz, [Ph$_2$C=P-P{C(**C**H$_3$)$_2$}-AgCl]$_2$) ppm.

^{31}P{^{1}H} NMR (162 MHz, CDCl$_3$, 298 K) δ 223.77 (d, J_{P-P} = 291.4 Hz, [Ph$_2$C=**P**-P(*t*Bu$_2$)-AgCl]$_2$), 51.93 (ddd, J_{P-P} = 291.4 Hz, $^1J(^{107}Ag-^{31}P)$ = 582.9 Hz, $^1J(^{109}Ag-^{31}P)$ = 627.8 Hz, [Ph$_2$C=P-**P**(*t*Bu$_2$)-AgCl]$_2$) ppm.

2.2.2. Synthesis of [(*p*-MeO-Ph)$_2$C=P-P*t*Bu$_2$-AgCl]$_2$ (Ag2).

(*p*-MeO-Ph)$_2$C=P-P*t*Bu$_2$ (100 mg, 0.248 mmol) was weighed together with AgCl (36 mg, 0.248 mmol) in a Schlenk tube, and then 10 mL of THF was added. The reaction solution was mixed for 24 hours. After this time, the initially red–orange solution changed to brown–yellow. Additionally, cloudiness in the solution was observed. The solution was evaporated under vacuum, and then 15 mL of toluene was added. After filtration, the clear orange solution was concentrated to 10 mL and stored at +4°C. After 24 hours, yellow crystals characterized as **Ag2** appeared (183 mg, yield 68%). Calculated elemental analysis (%) for C$_{42}$H$_{56}$Cl$_2$O$_4$P$_4$Ag$_2$: C, 48.72; H, 5.45. Found: C, 48.61; H, 5.60; melting point: 223-224°C.

^{1}H NMR (400 MHz, CDCl$_3$, 298 K) δ 7.35, 6.98, 6.75, (16H, [(*p*-MeO-**Ph**)$_2$C=P-P(*t*Bu$_2$)-AgCl]$_2$ – H$_{Ar}$), 3.91 (s, 6H, [(*p*-**Me**O-Ph)$_2$C=P-P(*t*Bu$_2$)-AgCl]$_2$), 3.75 (s, 6H, [(*p*-**Me**O-Ph)$_2$C=P-P(*t*Bu$_2$)-AgCl]$_2$), 1.31 (d, J_{P-H} = 14.9 Hz, 36 H, [(*p*-MeO-Ph)$_2$C=P-P(***t*Bu$_2$**)-AgCl]$_2$) ppm.

^{13}C{^{1}H} NMR (100.6 MHz, CDCl$_3$, 298 K) δ 208.90 (dd, J_{P-C} = 58.2, J_{P-C} = 3.0 Hz, [(*p*-MeO-Ph)$_2$**C**=P-P(*t*Bu$_2$)-AgCl]$_2$), 162.54 (d, J_{P-C} = 4.7 Hz, [(*p*-MeO-**Ph**)$_2$C=P-P(*t*Bu$_2$)-AgCl]$_2$ – C$_{Ar}$), 160.68 (s, [(*p*-MeO-**Ph**)$_2$C=P-P(*t*Bu$_2$)-AgCl]$_2$ – C$_{Ar}$), 138.72 (dd, J_{P-C} = 27.5, J_{P-C} = 8.3 Hz, [(*p*-MeO-**Ph**)$_2$C=P-P(*t*Bu$_2$)-AgCl]$_2$ – C$_{Ar}$), 135.11 (dd, J_{P-C} = 13.3, J_{P-C} = 9.9 Hz, [(*p*-MeO-**Ph**)$_2$C=P-

P(*t*Bu$_2$)-AgCl]$_2$ – C$_{Ar}$), 129.34 (dd, $J_{P\text{-}C}$ = 5.8, $J_{P\text{-}C}$ = 1.5 Hz, [(*p*-MeO-**Ph**)$_2$C=P-P(*t*Bu$_2$)-AgCl]$_2$ – C$_{Ar}$), 129.18 (d, $J_{P\text{-}C}$ = 20.7 Hz, [(*p*-MeO-**Ph**)$_2$C=P-P(*t*Bu$_2$)-AgCl]$_2$ – C$_{Ar}$), 115.13 (s, [(*p*-MeO-**Ph**)$_2$C=P-P(*t*Bu$_2$)-AgCl]$_2$ – C$_{Ar}$), 113.84 (s, [(*p*-MeO-**Ph**)$_2$C=P-P(*t*Bu$_2$)-AgCl]$_2$ – C$_{Ar}$), 77.12 (t, CDCl$_3$), 55.71 (s, [(*p*-**Me**O-Ph)$_2$C=P-P(*t*Bu$_2$)-AgCl]$_2$), 55.50 (s, [(*p*-**Me**O-Ph)$_2$C=P-P(*t*Bu$_2$)-AgCl]$_2$), 36.37 (dd, $J_{P\text{-}C}$ = 7.5 Hz, $J_{P\text{-}C}$ = 3.3 Hz, [(*p*-MeO-Ph)$_2$C=P-P{**C**(CH$_3$)$_2$}-AgCl]$_2$), 31.27 (dd, $J_{P\text{-}C}$ = 8.5 Hz, $J_{P\text{-}C}$ = 3.9 Hz, [(*p*-MeO-Ph)$_2$C=P-P{**C**(CH$_3$)$_2$}-AgCl]$_2$) ppm.

^{31}P{^{1}H} NMR (162 MHz, CDCl$_3$, 298 K) δ 206.97 (dd, $J_{P\text{-}P}$ = 294.7 Hz, ^2J(Ag-^{31}P) = 11.7 Hz, [(*p*-MeO-Ph)$_2$C=**P**-P(*t*Bu$_2$)-AgCl]$_2$), 52.41 (ddd, $J_{P\text{-}P}$ = 294.7 Hz, ^1J(^{107}Ag-^{31}P) = 590.5 Hz, ^1J(^{109}Ag-^{31}P) = 625.4 Hz, [(*p*-MeO-Ph)$_2$C=P-**P**(*t*Bu$_2$)-AgCl]$_2$) ppm.

2.3. Reactions of Ph$_2$C=P-P*t*Bu$_2$ or (*p*-MeO-Ph)$_2$C=P-P*t*Bu$_2$ with (tht)AuCl.

2.3.1. Synthesis of [Ph$_2$C=P-P(*t*Bu$_2$)-AuCl] (Au1).

Ph$_2$C=P-P*t*Bu$_2$ (100 mg, 0.292 mmol) was weighed together with (tht)AuCl (94 mg, 0.292 mmol) in a Schlenk tube and placed in a cooling bath. Next, 10 mL of THF was added, and almost immediately, the color changed from orange to orange–green. After three hours, the solution was removed from the cooling bath, and the solvent was evaporated. The oily residue was treated with 15 mL of toluene, and the mixture was filtered and concentrated to 2-3 mL of its volume. The solution was left at ambient temperature for 24 hours. After this time, colorless crystals appeared and were characterized as **Au1** (104 mg, yield 62%). Calculated elemental analysis (%) for C$_{21}$H$_{28}$Cl$_1$P$_2$Au$_1$: C, 43.88; H, 4.91. Found: C, 43.67; H, 5.02; melting point: 130-131°C.

^{1}H NMR (400 MHz, C$_6$D$_6$, 298 K) δ 7.52-6.92 (10H, [**Ph**$_2$C=P-P(*t*Bu$_2$)-AuCl] – H$_{Ar}$), 1.09 (d, $J_{P\text{-}H}$ = 15.4 Hz, 18 H, [(*p*-MeO-Ph)$_2$C=P-P(***t*Bu$_2$**)-AuCl]) ppm.

^{13}C{^{1}H} NMR (100.6 MHz, C$_6$D$_6$, 298 K) δ 210.80 (dd, $J_{P\text{-}C}$ = 58.1 Hz, $J_{P\text{-}C}$ = 6.4 Hz, [Ph$_2$**C**=P-P(*t*Bu$_2$)-AuCl], 145.46 (dd, $J_{P\text{-}C}$ = 28.2 Hz, $J_{P\text{-}H}$ = 10.9 Hz, [**Ph**$_2$C=P-P(*t*Bu$_2$)-AuCl – C$_{Ar}$), 143.34 (dd, $J_{P\text{-}C}$ = 13.6 Hz, $J_{P\text{-}H}$ = 10.9 Hz, [**Ph**$_2$C=P-P(*t*Bu$_2$)-AuCl – C$_{Ar}$), 131.00 (d, $J_{P\text{-}C}$ = 4.5

Hz,[**Ph**$_2$C=P-P(*t*Bu$_2$)-AuCl] – C$_{Ar}$), 129.56 (d, J_{P-C} = 0.9 Hz, [**Ph**$_2$C=P-P(*t*Bu$_2$)-AuCl] – C$_{Ar}$), 128.36 (d, J_{P-C} = 14.5 Hz, [**Ph**$_2$C=P-P(*t*Bu$_2$)-AuCl] – C$_{Ar}$), 128.31 (d, J_{P-C} = 8.2 Hz, [**Ph**$_2$C=P-P(*t*Bu$_2$)-AuCl] – C$_{Ar}$), 38.14 (dd, J_{P-C} = 19.1 Hz, J_{P-H} = 5.4 Hz, [Ph$_2$C=P-P{**C**(CH$_3$)$_2$}-AuCl]), 30.47 (dd, J_{P-C} = 5.4 Hz, J_{P-H} = 4.5 Hz, [Ph$_2$C=P-P{C(**C**H$_3$)$_2$}-AuCl]) ppm.

^{31}P{^{1}H} NMR (162 MHz, C$_6$D$_6$, 298 K) δ 200.78 (d, J_{P-P} = 321.2 Hz, [Ph$_2$C=**P**-P(*t*Bu$_2$)-AuCl]), 66.96 (d, J_{P-P} = 321.2 Hz, [Ph$_2$C=P-**P**(*t*Bu$_2$)-AuCl]) ppm.

2.3.2. Synthesis of [(*p*-MeO-Ph)$_2$C=P-P(*t*Bu$_2$)-AuCl] (Au2).

(*p*-MeO-Ph)$_2$C=P-P*t*Bu$_2$ (50 mg, 0.124 mmol) was weighed together with (tht)AuCl (40 mg, 0.124 mmol) in a Schlenk tube and placed in a cooling bath. Next, 5 mL of THF was added, and almost immediately, the color changed from dark–orange to brown. After three hours, the solution was removed from the cooling bath, and the solvent was evaporated. The oily residue was treated with 0.7 mL of toluene-d$_8$ and transferred to an NMR tube.

^{1}H NMR (400 MHz, C$_6$D$_6$, 298 K) δ 7.78-6.52 (8H, [(*p*-MeO-**Ph**)$_2$C=P-P(*t*Bu$_2$)-AuCl] – H$_{Ar}$), 3.68 (s, 6H, [(*p*-**Me**O-Ph)$_2$C=P-P(*t*Bu$_2$)-AuCl], 3.16 (s, 3H, [(*p*-**Me**O-Ph)$_2$C=P-P(*t*Bu$_2$)-AuCl]), 1.07 (d, J_{P-H} = 15.4 Hz, 18 H, [(*p*-MeO-Ph)$_2$C=P-P(***t*Bu$_2$**)-AuCl]), 3.57 and 1.36 (THF protons) ppm.

^{13}C{^{1}H} NMR (100.6 MHz, C$_6$D$_6$, 298 K) δ 209.88 (dd, J_{P-C} = 59.4, J_{P-C} = 7.3 Hz, [(*p*-MeO-Ph)$_2$**C**=P-P(*t*Bu$_2$)-AuCl]), 163.01 (d, J_{P-C} = 4.5 Hz, [(*p*-MeO-**Ph**)$_2$C=P-P(*t*Bu$_2$)-AuCl] – C$_{Ar}$), 161.64 (s, [(*p*-MeO-**Ph**)$_2$C=P-P(*t*Bu$_2$)-AuCl] – C$_{Ar}$), 138.99 (dd, J_{P-C} = 28.6, J_{P-C} = 10.4 Hz, [(*p*-MeO-**Ph**)$_2$C=P-P(*t*Bu$_2$)-AuCl] – C$_{Ar}$), 135.82 (dd, J_{P-C} = 13.62, J_{P-C} = 9.1 Hz, [(*p*-MeO-**Ph**)$_2$C=P-P(*t*Bu$_2$)-AuCl] – C$_{Ar}$), 132.45 (d, J_{P-C} = 0.9 Hz, [(*p*-MeO-**Ph**)$_2$C=P-P(*t*Bu$_2$)-AuCl] – C$_{Ar}$), 130.45 (d, J_{P-C} = 5.4 Hz, [(*p*-MeO-**Ph**)$_2$C=P-P(*t*Bu$_2$)-AuCl] – C$_{Ar}$), 115.34 (s, [(*p*-MeO-**Ph**)$_2$C=P-P(*t*Bu$_2$)-AuCl] – C$_{Ar}$), 113.77 (s, [(*p*-MeO-**Ph**)$_2$C=P-P(*t*Bu$_2$)-AuCl] – C$_{Ar}$), 55.23 (s, [(*p*-**Me**O-Ph)$_2$C=P-P(*t*Bu$_2$)-AuCl]), 54.75 (s, [(*p*-**Me**O-Ph)$_2$C=P-P(*t*Bu$_2$)-AuCl]), 38.23 (dd, J_{P-C} = 18.2 Hz, J_{P-C} = 5.4

Hz, [(*p*-MeO-Ph)$_2$C=P-P{**C**(CH$_3$)$_2$}-AuCl]), 30.55 (dd, J_{P-C} = 5.4 Hz, J_{P-C} = 4.5 Hz, [(*p*-MeO-Ph)$_2$C=P-P{**C**(CH$_3$)$_2$}-AuCl]) ppm.

^{31}P{^{1}H} NMR (162 MHz, C_6D_6, 298 K) δ 199.77 (d, J_{P-P} = 330.9 Hz, [(*p*-MeO-Ph)$_2$C=**P**-P(*t*Bu$_2$)-AuCl], 68.53 (d, J_{P-P} = 330.9 Hz, [(*p*-MeO-Ph)$_2$C=P-**P**(*t*Bu$_2$)-AuCl]) ppm.

3.4. General method of stability study.

Complexes **Cu1**, **Cu2**, **Ag1** and **Ag2** (100 mg) were put into Schlenk flasks (**Cu1**: 0.113 mmol; **Cu2**: 0.084 mmol; **Ag1**: 0.103 mmol; **Ag2**: 0.092 mmol) and thermolyzed at 400°C for 30 min. After heating, the obtained black powders were washed at room temperature with three portions of THF (3 x 10 mL) and dried under vacuum. The following amounts were obtained: **Cu1**, 15 mg; **Cu2**, 17 mg; **Ag1**, 24 mg; and **Ag2**, 26 mg. Black powders were tested by EDX.

PART B. X-RAY CRYSTALLOGRAPHIC DATA

The X-ray intensity data for **Cu1**, **Cu2**, **Ag1**, **Ag2**, **Au1** were measured with an IPDS2T diffractometer equipped with an IPDS2T STOE image plate detector system and microfocus X-ray sources providing Kα radiation by high-grade multilayer X-ray mirror optics for Mo (λ = 0.71073 Å) wavelengths. The all measurements were carried out at 120 K. The structures of the compounds were solved by direct methods and refined against F^2 with the Shelxs-2008 and Shelxl-2008 programs[1] run under WinGX.[2] Non-hydrogen atoms were refined with anisotropic displacement parameters. The isotropic displacement parameters of all hydrogens were fixed to 1.2 U_{eq} for CH, CH_2 and aromatic (1.5 times for methyl groups).

The crystallographic data for the structures of **Cu1**, **Cu2**, **Ag1**, **Ag2**, **Au1** reported in this paper have been deposited in the Cambridge Crystallographic Data Centre as supplementary publication No. CCDC 2194197-2194201. Copies of the data can be obtained free of charge upon application to the CCDC, 12 Union Road, Cambridge CB2 1EZ, UK (Fax: (+44) 1223-336-033; E mail: deposit@ccdc.cam.ac.uk).

Table S1. Crystallographic data for **Cu1, Cu2, Ag1**.

	Cu1	**Cu2**	**Ag1**
Empirical formula	$C_{21}H_{28}Cl_1Cu_1P_2$	$C_{60}H_{80}Cu_2Cl_2O_4P_4$	$C_{42}H_{56}Ag_2Cl_2P_4$
Formula weight	441.36	1187.1	971.38
Radiation source	Mo-*K*α	Mo-*K*α	Mo-*K*α
Wavelength [Å]	0.71073	0.71073	0.71073
Crystal System	triclinic	triclinic	triclinic
Space group	*P*-1	*P*-1	*P*-1
a [Å]	9.0536(9)	9.6767(9)	9.0194(6)
b [Å]	9.0454(9)	10.2025(6)	9.2693(7)
c [Å]	14.6284(18)	15.7136(9)	14.8213(12)
α [°]	76.264(9)	105.628(5)	75.449(6)
β [°]	73.160(9)	94.666(6)	75.801(6)
γ [°]	67.682(8)	97.674(6)	66.277(5)
V [Å^3]	4168.4(3)	1469.39(19)	1083.38(15)
Z	2	1	1
Calculated Density [g·cm^{-1}]	1.396	1.342	1.489
T [K]	120(2)	120(2)	120(2)
μ [mm^{-1}]	1.322	0.968	1.200
Theta range for data collection [°]	2.46-26.93	2.14-29.51	2.44-29.43
Index ranges	-11<=h<=11 -11<=k<=11 -19<=l<=19	-12<=h<=12 -12<=k<=13 -20<=l<=20	-11<=h<=11 -11<=k<=11 -18<=l<=18
Data / restraints / parameters	5015/0/232	7023/0/375	4682/0/233
Goodness-of-fit on F^2	0.978	0.983	1.038
Final R indices	0.0916	0.0338	0.0918
[*I*>2σ(I)]	0.1884	0.0530	0.1188
R indices (all data)	0.2199	0.0770	0.2563
[*I*>2σ(I)] (all data)	0.2755	0.0813	0.2796
Largest diff. peak and hole [e.Å^{-3}]	0.891 and -1.026	0.454 and -0.378	2.623 and -1.528
CCDC	**2194199**	**2194200**	**2194198**

Table S2. Crystallographic data for **Ag2** and **Au1**.

	Ag2	**Au1**
Empirical formula	$C_{42}H_{64}Ag_2Cl_2O_4P_4$	$C_{21}H_{28}AuClP_2$
Formula weight	1091.49	574.79
Radiation source	Mo-*K*α	Mo-*K*α
Wavelength [Å]	0.71073	0.71073
Crystal System	Monoclinic	Monoclinic
Space group	$P2_1/c$	$P2_1/c$
a [Å]	15.8278(7)	16.9857(6)
b [Å]	15.4563(5)	7.4820(3)
c [Å]	20.4611(8)	16.8471(6)
α [°]	90	90
β [°]	103.735(3)	95.629(3)
γ [°]	90	90
V [Å^3]	4862.4(3)	2130.72(14)
Z	4	4
Calculated Density [g·cm^{-1}]	1.491	1.792
T [K]	120(2)	120(2)
μ [mm^{-1}]	1.087	7.182
Theta range for data collection [°]	2.28-29.25	2.41-29.59
Index ranges	-17<=h<=20 -20<=k<=20 -27<=l<=26	-23<=h<=23 -10<=k<=8 -23<=l<=20
Data / restraints / parameters	11683/0/521	5718/0/232
Goodness-of-fit on F^2	0.947	1.098
Final R indices	0.0611	0.0281
[*I*>2σ(I)]	0.1580	0.0670
R indices (all data)	0.0962	0.0347
[*I*>2σ(I)] (all data)	0.1197	0.0719
Largest diff. peak and hole [e.Å^{-3}]	0.731 and -0.665	2.432 and -1.573
CCDC	**2194197**	**2194201**

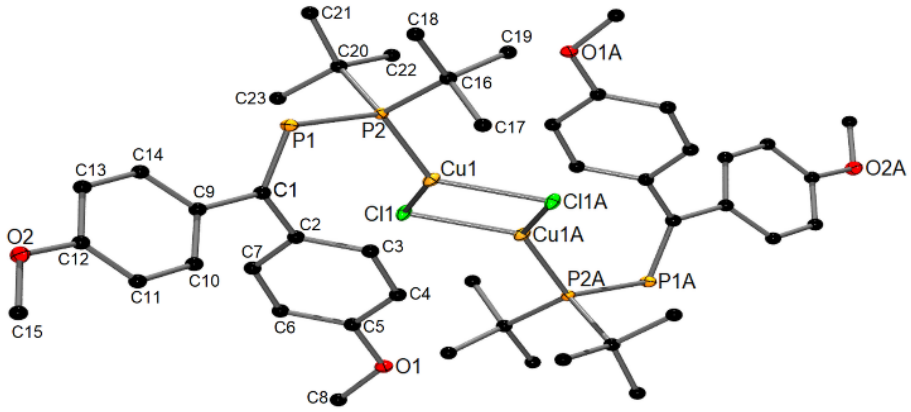

Figure S1. The molecular structure of **Cu1** (ellipsoids are drawn at the 50% probability level; hydrogen atoms have been omitted for clarity; equivalent position invoked by the additional A letters in the atom labels: -x, 1-y, -z). Important distances (Å) and angles (deg): P1-P2 2.2135(7), P1-C1 1.7008(19), P2-Cu1 2.2024(5), Cu1-Cl1 2.2990(5), Cu1-Cl1A 2.3431(6), Cu1-Cu1A 3.0356(5); C1-P1-P2 108.26(7), P1-P2-Cu1 123.46(3), P2-Cu1-Cl1 130.61(2), and Cl1-Cu1-Cl1A 98.330(18), ΣCu1 = 354.21(10).

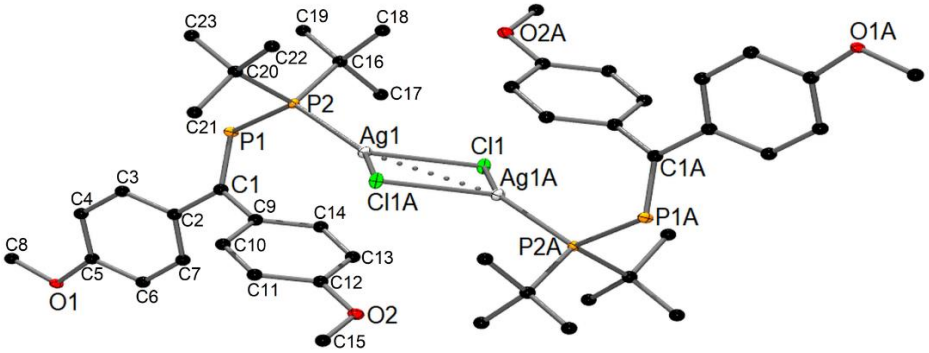

Figure S2. The molecular structure of **Ag2** (first molecule) (ellipsoids are drawn at the 50% probability level; hydrogen atoms have been omitted for clarity; equivalent position invoked by the additional A letters in the atom labels: 2-x, 2-y, 1-z). Important distances (Å) and angles (deg): P1-P2 2.211(2), P3-P4 2.225(2), P1-C1 1.683(6), P3-C24 1.698(6), P2-Ag1 2.3976(16), P4-Ag2 2.3865(14), Ag1-Cl1 2.5059(15), Ag1-Cl1A 2.6047(14), Ag2-Cl2 2.4197(15), Ag2-Cl2A 2.8188(15), Ag1-Ag1A 3.2658(15); C1-P1-P2 106.5(2), C24-P3-P4 109.6(2), P1-P2-Ag1 123.52(8), P3-P4-Ag2 122.68(7), P2-Ag1-Cl1 137.30(5), P4-Ag2-Cl2 157.44(6), Cl1-Ag1-Cl1A 95.20(4), and Cl2-Ag2-Cl2A 90.23(5), ΣAg1 = 356.63(5).

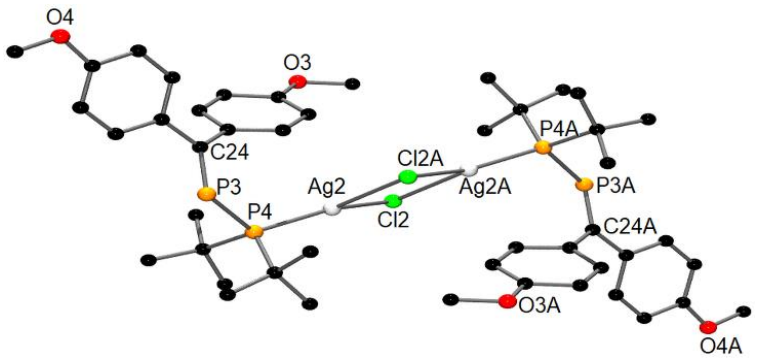

Figure S3. The molecular structure of **Ag2** (second molecule) (ellipsoids are drown at the 50% probability level; hydrogen atoms have been omitted for clarity; equivalent position invoked by the additional A letters in the atom labels: 1-x, 1-y, 1-z). Important distances (Å) and angles (deg): P3-P4 2.225(2), P3-C24 1.698(6), P4-Ag2 2.3865(14), Ag2-Cl2 2.4197(15), Ag2-Cl2A 2.8188(15), Ag2-Ag2A 3.7076(6); C24-P3-P4 109.6(2), P3-P4-Ag2 122.68(7), P4-Ag2-Cl2 157.44(6), Cl2-Ag2-Cl2A 90.23(5), ΣAg2 = 359.25(5).

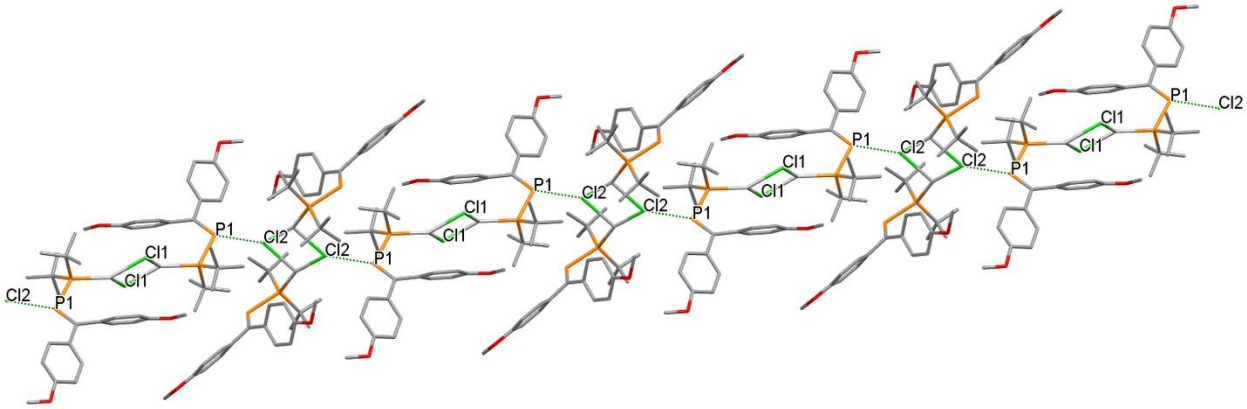

Figure S4. Arrangement of molecules in the crystal of **Ag2**.

PART C. NMR SPECTUM SECTION

1. Reactions of phosphanylphosphaalkenes with CuCl

1.1. Reaction of Ph_2C=P-P*t*Bu_2 with CuCl.

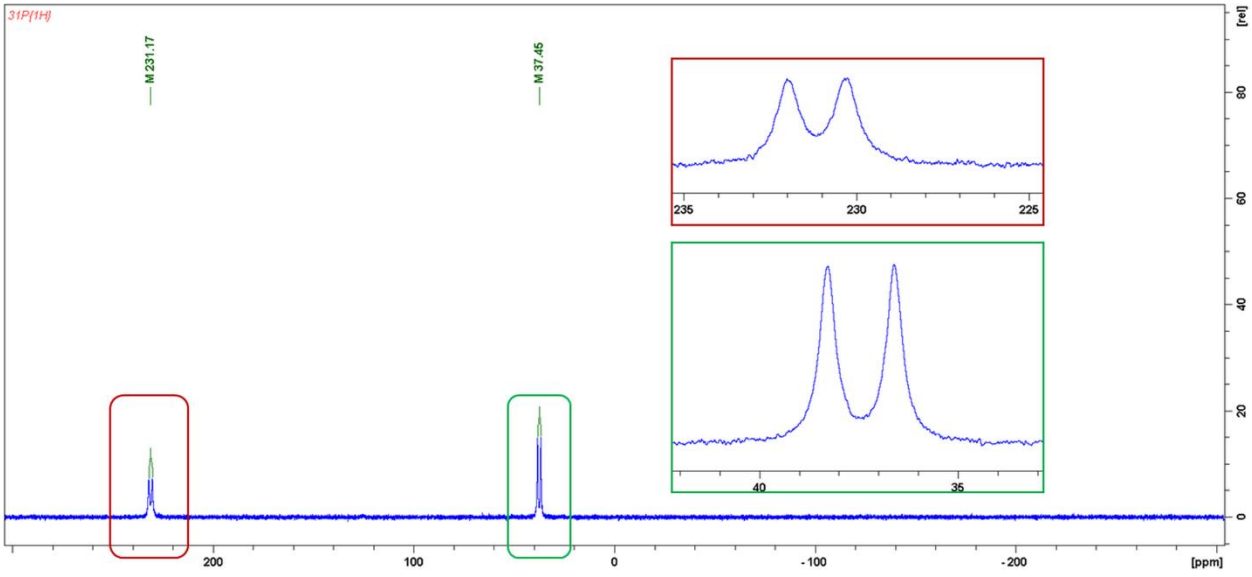

Figure S5. $^{31}P\{^{1}H\}$ NMR ($CDCl_3$, 162 MHz) spectrum of [Ph_2C=P-P(*t*Bu_2)-CuCl]$_2$ (**Cu1**).

- 231.17 ppm, d, $J_{P\text{-}P}$ = 268.7 Hz, [Ph_2C=**P**-P(*t*Bu_2)-CuCl]$_2$;
- 37.44 ppm, d, $J_{P\text{-}P}$ = 268.7 Hz, [Ph_2C=P-**P**(*t*Bu_2)-CuCl]$_2$;

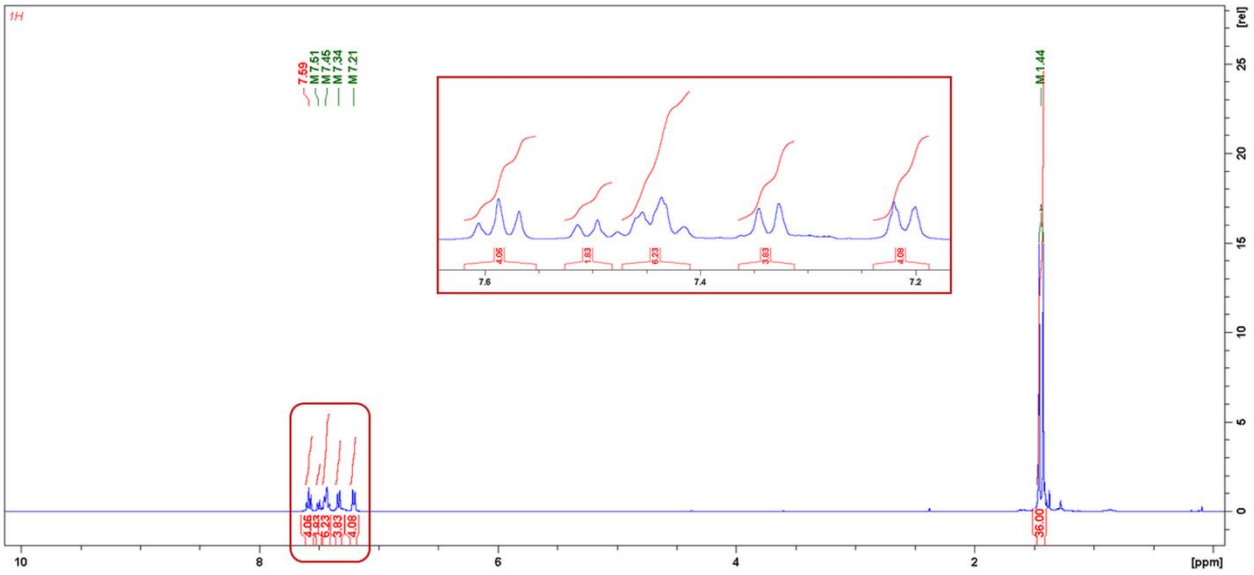

Figure S6. ^{1}H NMR ($CDCl_3$, 400 MHz) spectrum of $[Ph_2C{=}P\text{-}P(tBu_2)\text{-}CuCl]_2$ (**Cu1**).

- 7.59, 7.51, 7.45, 7.32 and 7.21 ppm, 20H, $[\mathbf{Ph}_2C{=}P\text{-}P(tBu_2)\text{-}CuCl]_2$ – H_{Ar};
- 1.44 ppm, d, $J_{P\text{-}H}$ = 14.1 Hz, 36 H, $[Ph_2C{=}P\text{-}P(\mathbf{\textit{t}Bu}_2)\text{-}CuCl]_2$;

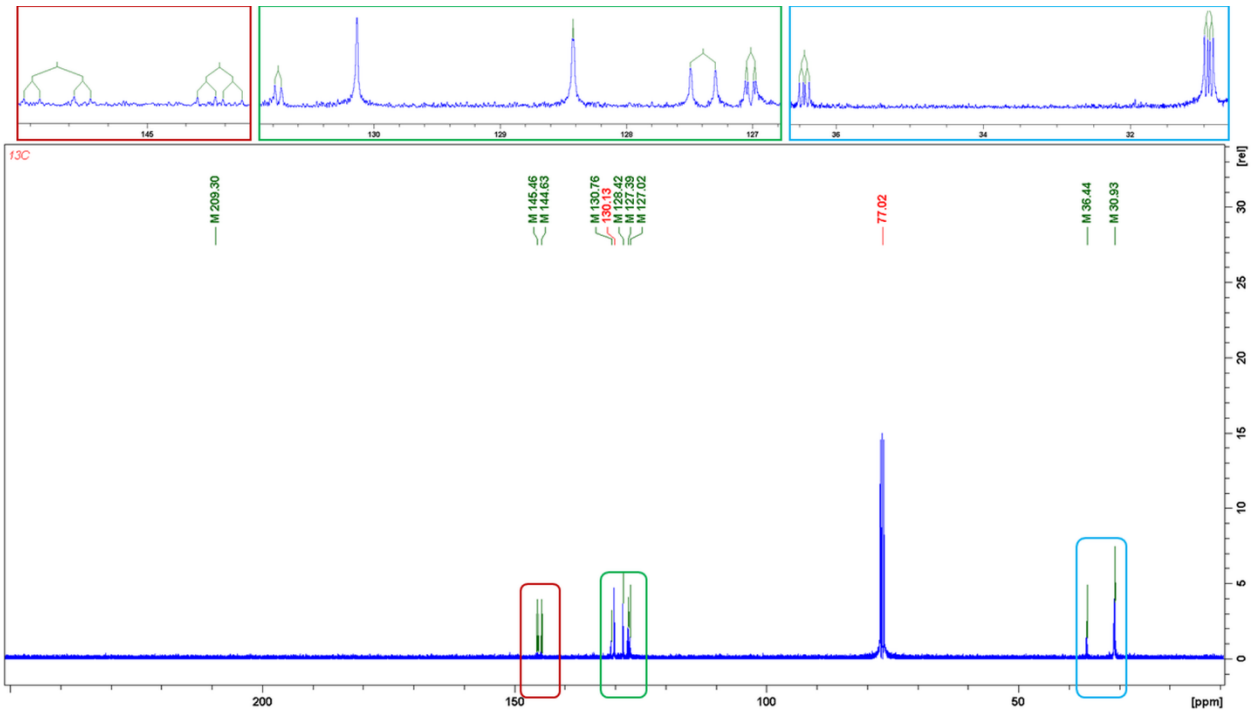

Figure S7. $^{13}C\{^{1}H\}$ NMR ($CDCl_3$, 100.6 MHz) spectrum of $[Ph_2C{=}P\text{-}P(tBu_2)\text{-}CuCl]_2$ (**Cu1**).

- 209.3 ppm, d, $J_{P\text{-}C}$ = 60.2 Hz, $[Ph_2\mathbf{C}{=}P\text{-}P(tBu_2)\text{-}CuCl]_2$ – very weak signal located according to the $^{13}C\{^{1}H\}/^{1}H$-HMBC NMR spectrum;
- 145.46 ppm, dd, $J_{P\text{-}C}$ = 25.9 Hz, $J_{P\text{-}H}$ = 8.1 Hz, $[\mathbf{Ph}_2C{=}P\text{-}P(tBu_2)\text{-}CuCl]_2 - C_{Ar}$;
- 144.63 ppm, dd, $J_{P\text{-}C}$ = 13.6 Hz, $J_{P\text{-}H}$ = 9.7 Hz, $[\mathbf{Ph}_2C{=}P\text{-}P(tBu_2)\text{-}CuCl]_2 - C_{Ar}$;
- 130.76 ppm, d, $J_{P\text{-}C}$ = 5.0 Hz, $[\mathbf{Ph}_2C{=}P\text{-}P(tBu_2)\text{-}CuCl]_2 - C_{Ar}$;
- 130.13 ppm, s, $J_{P\text{-}C}$ = 5.0 Hz, $[\mathbf{Ph}_2C{=}P\text{-}P(tBu_2)\text{-}CuCl]_2 - C_{Ar}$;
- 128.42 ppm, d, $J_{P\text{-}C}$ = 0.9 Hz, $[\mathbf{Ph}_2C{=}P\text{-}P(tBu_2)\text{-}CuCl]_2 - C_{Ar}$;
- 127.39 ppm, d, $J_{P\text{-}C}$ = 20.0 Hz, $[\mathbf{Ph}_2C{=}P\text{-}P(tBu_2)\text{-}CuCl]_2 - C_{Ar}$;
- 127.02 ppm, dd, $J_{P\text{-}C}$ = 6.4 Hz, $J_{P\text{-}H}$ = 1.8 Hz, $[\mathbf{Ph}_2C{=}P\text{-}P(tBu_2)\text{-}CuCl]_2 - C_{Ar}$;
- 36.44 ppm, dd, $J_{P\text{-}C}$ = 8.0 Hz, $J_{P\text{-}H}$ = 5.5 Hz, $[Ph_2C{=}P\text{-}P\{\mathbf{C}(CH_3)_2\}\text{-}CuCl]_2$;
- 30.93 ppm, dd, $J_{P\text{-}C}$ = 6.44 Hz, $J_{P\text{-}H}$ = 1.8 Hz, $[Ph_2C{=}P\text{-}P\{C(\mathbf{C}H_3)_2\}\text{-}CuCl]_2$;

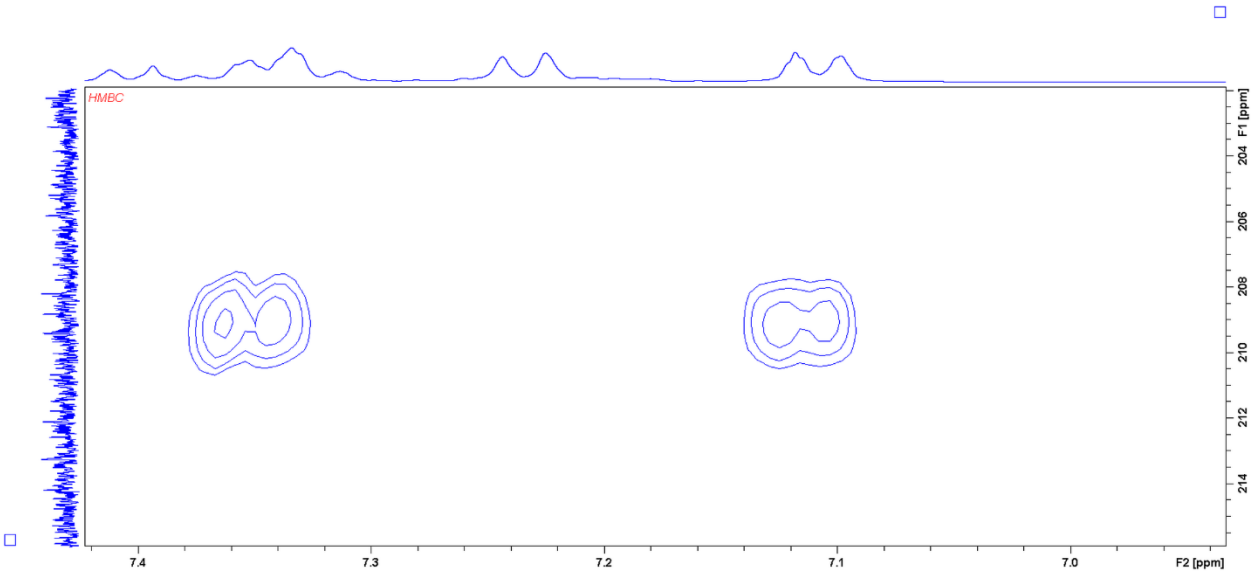

Figure S8. $^{13}C\{^{1}H\}/^{1}H$-HMBC NMR spectrum of **Cu1** presenting the correlation of aromatic protons and carbon atom of C=P bond system.

1.2. Reaction of (p-MeO-Ph)$_2$C=P-PtBu$_2$ with CuCl.

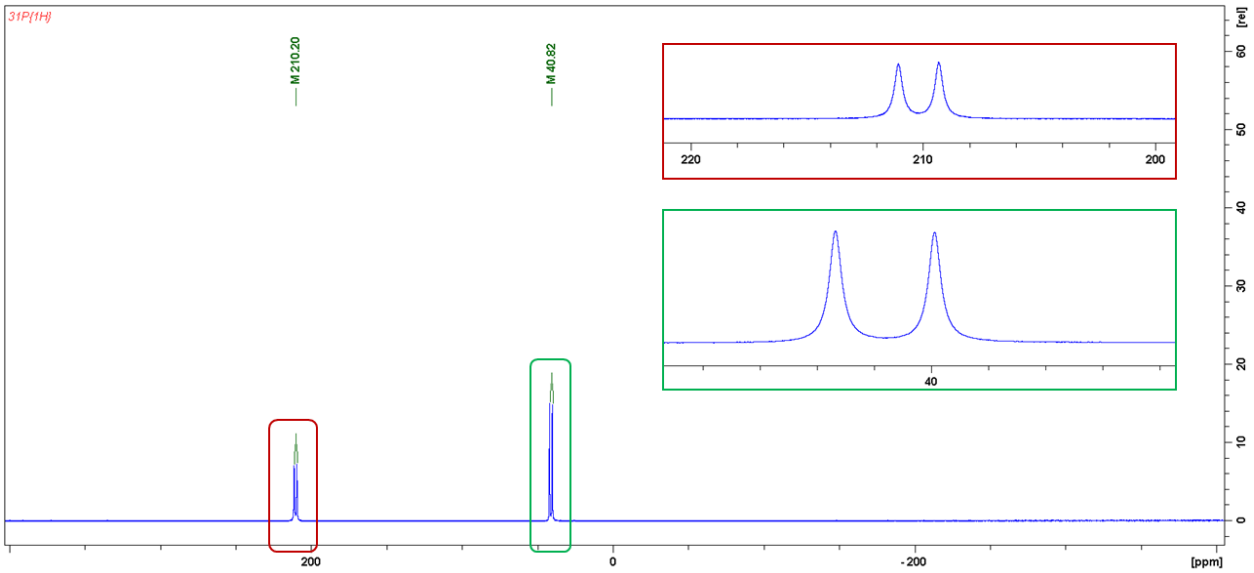

Figure S9. $^{31}P\{^{1}H\}$ NMR ($CDCl_3$, 162 MHz) spectrum of isolated [(p-MeO-Ph)$_2$C=**P**-P(tBu$_2$)-CuCl]$_2$ (**Cu2**).

- 210.20 ppm, d, $J_{P\text{-}P}$ = 280.7 Hz, [(p-MeO-Ph)$_2$C=**P**-P(tBu$_2$)-CuCl]$_2$;
- 40.82 ppm, d, $J_{P\text{-}P}$ = 280.7 Hz, [(p-MeO-Ph)$_2$C=P-**P**(tBu$_2$)-CuCl]$_2$;

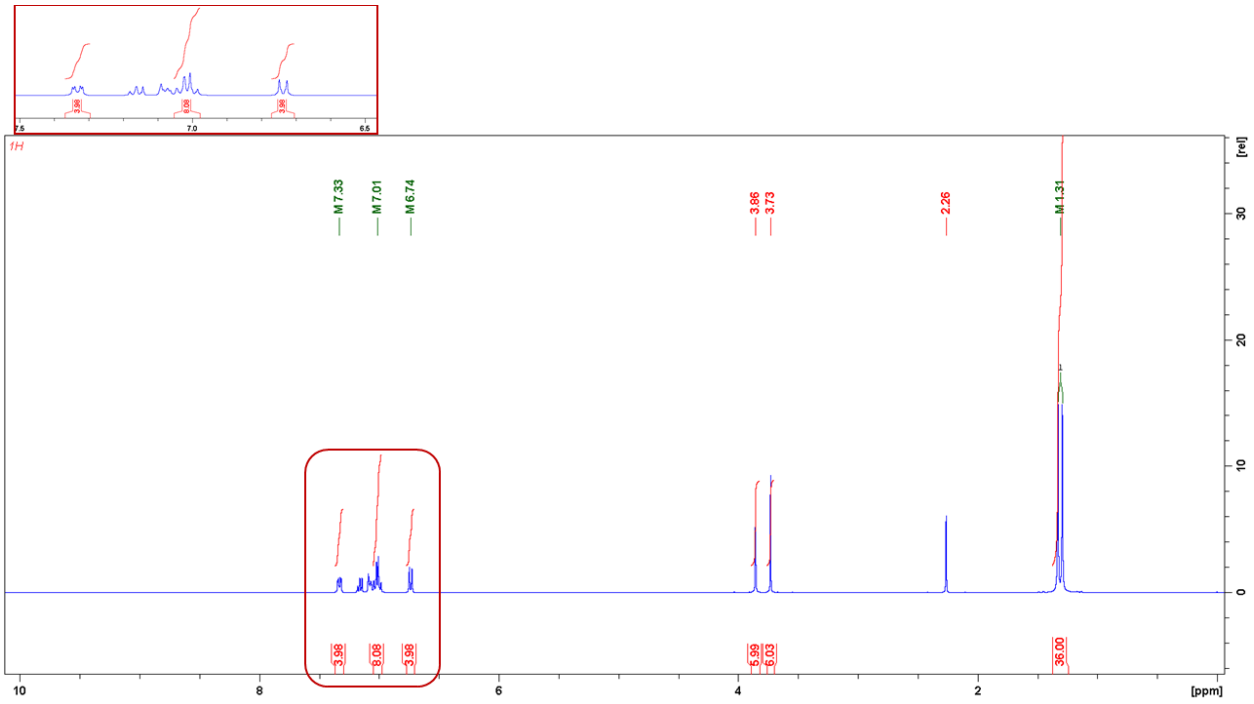

Figure S10. ^{1}H NMR ($CDCl_3$, 400 MHz) spectrum of isolated [(*p*-MeO-Ph)$_2$C=**P**-P(*t*Bu$_2$)-CuCl]$_2$ (**Cu2**).

- 7.33 ppm, 7.01 ppm, 6.74 ppm, 16H, [(*p*-MeO-**Ph**)$_2$C=P-P(*t*Bu$_2$)-CuCl]$_2$ – H_{Ar};
- from 7.20 to 7.05 ppm - aromatic protons of one molecule of toluene (present in the unit cell);
- 3.86 ppm, s, 3H, [(*p*-**M**eO-Ph)$_2$C=P-P(*t*Bu$_2$)-CuCl]$_2$;
- 3.73 ppm, s, 3H, [(*p*-**M**eO-Ph)$_2$C=P-P(*t*Bu$_2$)-CuCl]$_2$;
- 2.26 ppm, s, methyl group protons of one molecule of toluene (present in the unit cell);
- 1.31 ppm, d, $J_{P\text{-}H}$ = 14.2 Hz, 36 H, [(*p*-MeO-Ph)$_2$C=P-P(***t*Bu**$_2$)-CuCl]$_2$;

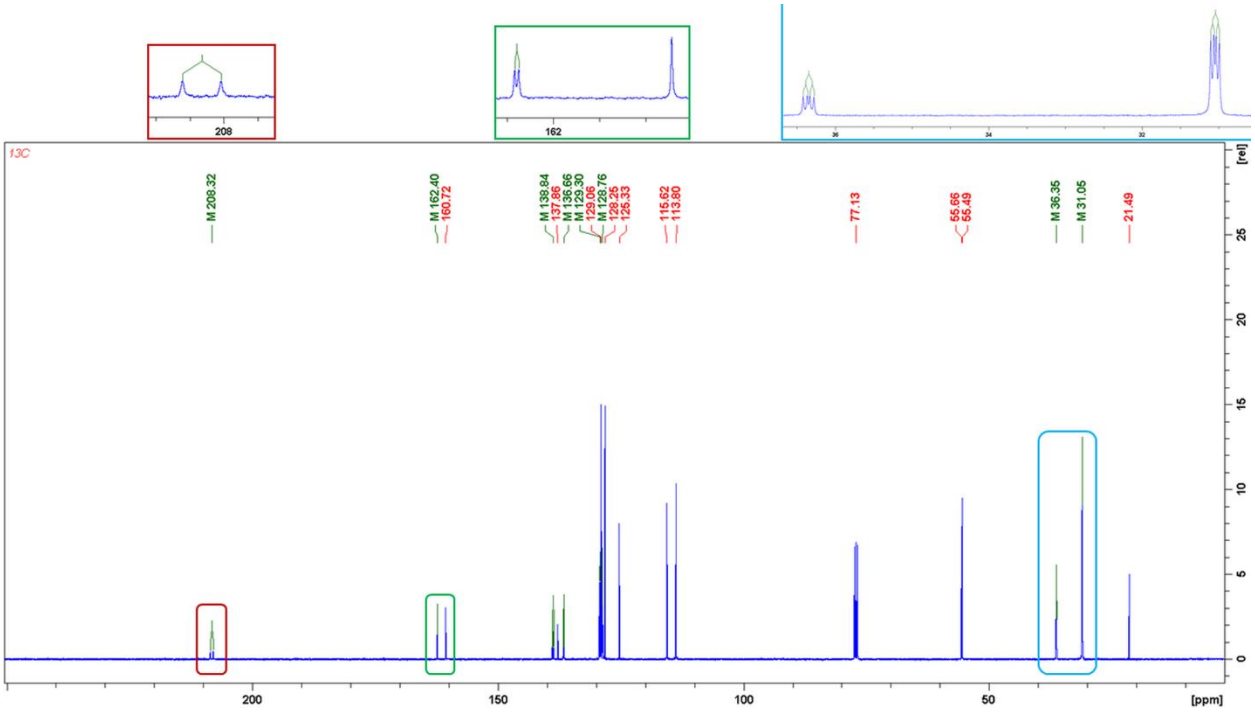

Figure S11. $^{13}C\{^{1}H\}$ NMR ($CDCl_3$, 100.6 MHz) spectrum of isolated [(*p*-MeO-Ph)$_2$C=**P**-P(*t*Bu$_2$)-CuCl]$_2$ (**Cu2**).

- 208.32 ppm, d, $J_{P\text{-}C}$ = 57.2 Hz, [(*p*-MeO-Ph)$_2$**C**=P-P(*t*Bu$_2$)-CuCl]$_2$;
- 162.40 ppm, d, $J_{P\text{-}C}$ = 4.4 Hz, [(*p*-MeO-**Ph**)$_2$C=P-P(*t*Bu$_2$)-CuCl]$_2$ – C_{Ar};
- 160.72 ppm, s, [(*p*-MeO-**Ph**)$_2$C=P-P(*t*Bu$_2$)-CuCl]$_2$ – C_{Ar};
- 138.84 ppm, dd, $J_{P\text{-}C}$ = 26.8 Hz, $J_{P\text{-}C}$ = 8.4 Hz, [(*p*-MeO-**Ph**)$_2$C=P-P(*t*Bu$_2$)-CuCl]$_2$ – C_{Ar};
- 137.86 ppm, s, toluene – C_{Ar};
- 136.66 ppm, dd, $J_{P\text{-}C}$ = 13.5 Hz, $J_{P\text{-}C}$ = 9.3 Hz, [(*p*-MeO-**Ph**)$_2$C=P-P(*t*Bu$_2$)-CuCl]$_2$ – C_{Ar};
- 129.30 ppm, d, $J_{P\text{-}C}$ = 19.9 Hz, [(*p*-MeO-**Ph**)$_2$C=P-P(*t*Bu$_2$)-CuCl]$_2$ – C_{Ar};
- 129.06 ppm, s, [(*p*-MeO-**Ph**)$_2$C=P-P(*t*Bu$_2$)-CuCl]$_2$ – C_{Ar};
- 128.76 ppm, dd, toluene – C_{Ar};
- 128.25 ppm, s, toluene – C_{Ar};
- 125.33 ppm, s, toluene – C_{Ar};
- 115.62 ppm, s, [(*p*-MeO-**Ph**)$_2$C=P-P(*t*Bu$_2$)-CuCl]$_2$ – C_{Ar};
- 113.80 ppm, s, [(*p*-MeO-**Ph**)$_2$C=P-P(*t*Bu$_2$)-CuCl]$_2$ – C_{Ar};
- 77.13 ppm, t, $CDCl_3$;
- 55.66 ppm, s, [(*p*-**Me**O-Ph)$_2$C=P-P{C(CH$_3$)$_2$}-CuCl]$_2$;
- 55.49 ppm, s, [(*p*-**Me**O-Ph)$_2$C=P-P{C(CH$_3$)$_2$}-CuCl]$_2$;
- 36.35 ppm, dd, $J_{P\text{-}C}$ = 8.6 Hz, $J_{P\text{-}C}$ = 5.4 Hz, [(*p*-MeO-Ph)$_2$C=P-P{**C**(CH$_3$)$_2$}-CuCl]$_2$;
- 31.05 ppm, dd, , $J_{P\text{-}C}$ = 8.6 Hz, $J_{P\text{-}C}$ = 5.4 Hz, [(*p*-MeO-Ph)$_2$C=P-P{C(**C**H$_3$)$_2$}-CuCl]$_2$;

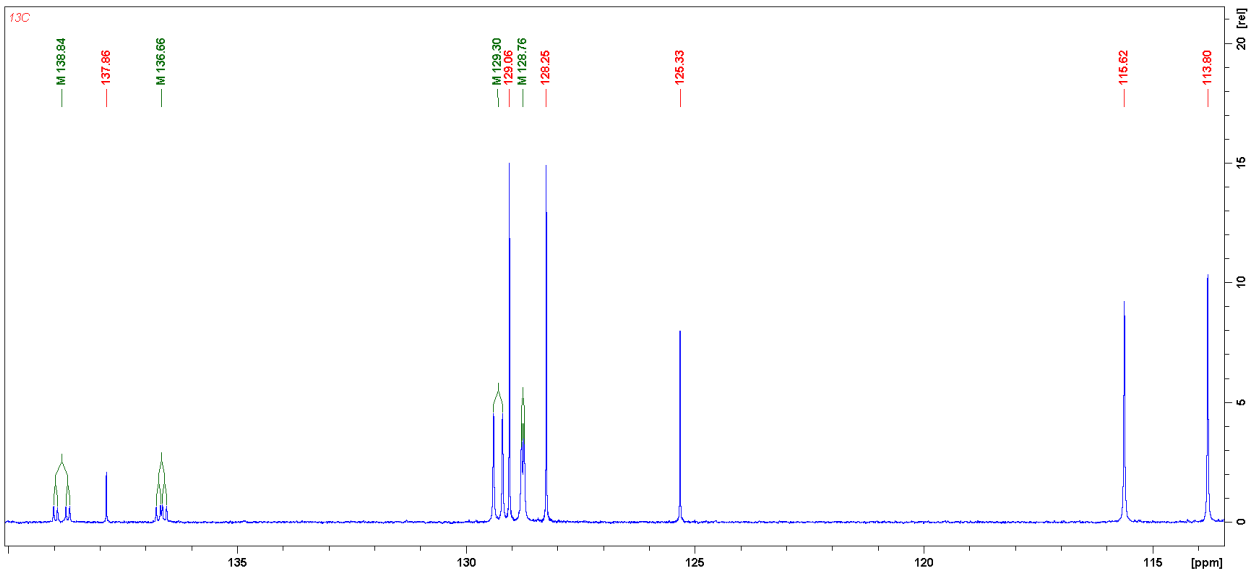

Figure S12. $^{13}C\{^{1}H\}$ NMR ($CDCl_3$, 100.6 MHz) spectrum of isolated [(*p*-MeO-Ph)$_2$C=**P**-P(*t*Bu$_2$)-CuCl]$_2$ (**Cu2**) in the range from 140 ppm to 110 ppm.

2. Reactions of phosphanylphosphaalkenes with AgCl

2.1 Reaction of Ph_2C=P-P*t*Bu_2 with AgCl.

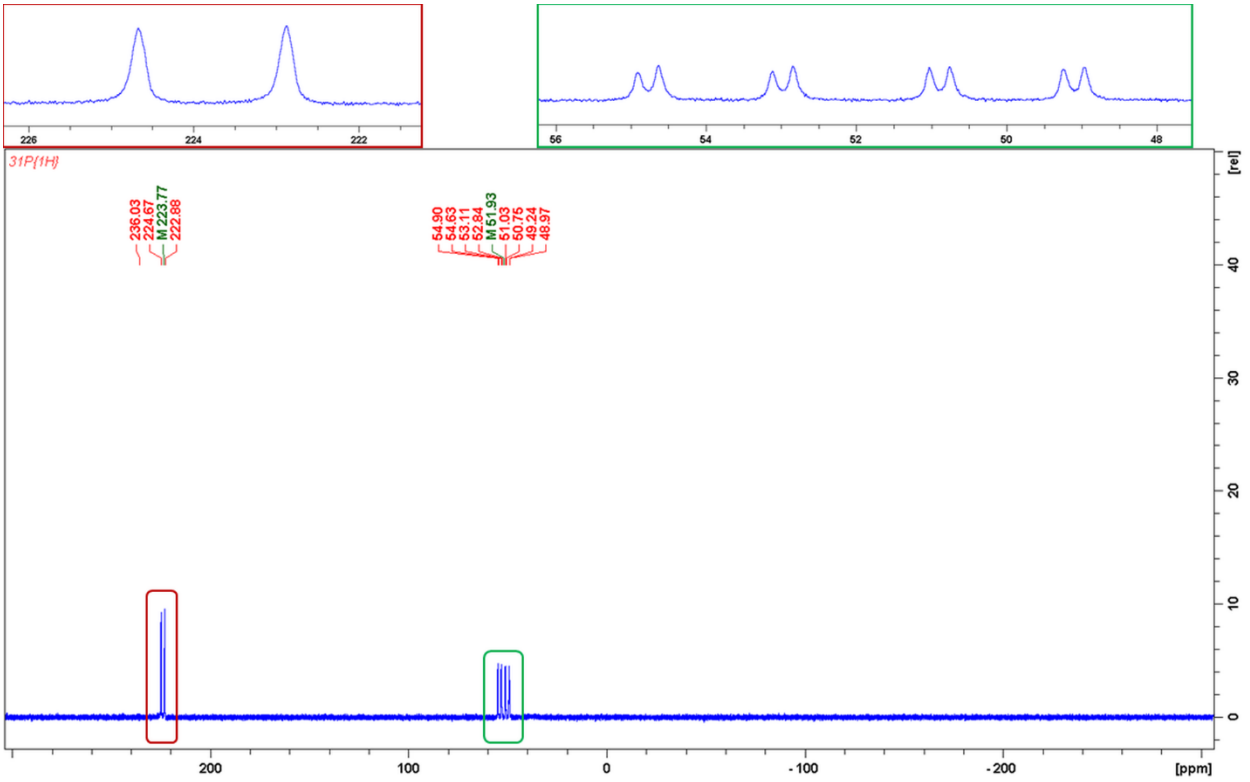

Figure S13. $^{31}P\{^{1}H\}$ NMR ($CDCl_3$, 162 MHz) spectrum of [Ph_2C=P-P-(*t*Bu_2)-AgCl]$_2$ (**Ag1**).

- 223.77 ppm, d, $J_{P\text{-}P}$ = 291.4 Hz, [Ph_2C=**P**-P(*t*Bu_2)-AgCl]$_2$, due to the low P-Ag coupling constants by two bonds and wide signals, P-Ag coupling constants are visible;
- 51.93, ddd, $J_{P\text{-}P}$ = 291.4 Hz, $^{1}J(^{107}Ag\text{-}^{31}P)$ = 582.9 Hz, $^{1}J(^{109}Ag\text{-}^{31}P)$ = 627.8 Hz, [Ph_2C=P-**P**(*t*Bu_2)-AgCl]$_2$;

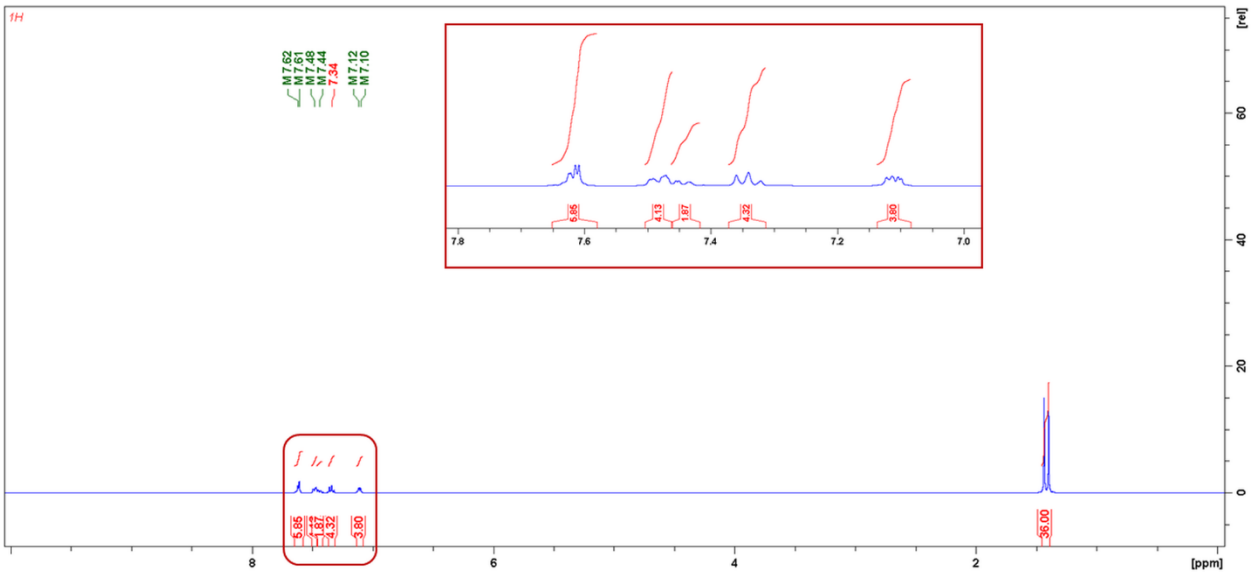

Figure S14. ^{1}H NMR ($CDCl_3$, 400 MHz) spectrum of isolated $[Ph_2C{=}P\text{-}P(tBu_2)\text{-}AgCl]_2$ (**Ag1**).

- 7.62, 7.61, 7.48, 7.44, 7.34, 7.12 and 7.10 ppm, 20H, $[\mathbf{Ph}_2C{=}P\text{-}P(tBu_2)\text{-}AgCl]_2$ – H_{Ar};
- 1.42 ppm, d, $J_{P\text{-}H}$ = 14.8 Hz, $[Ph_2C{=}P\text{-}P(\mathbf{\mathit{t}Bu_2})\text{-}AgCl]_2$;

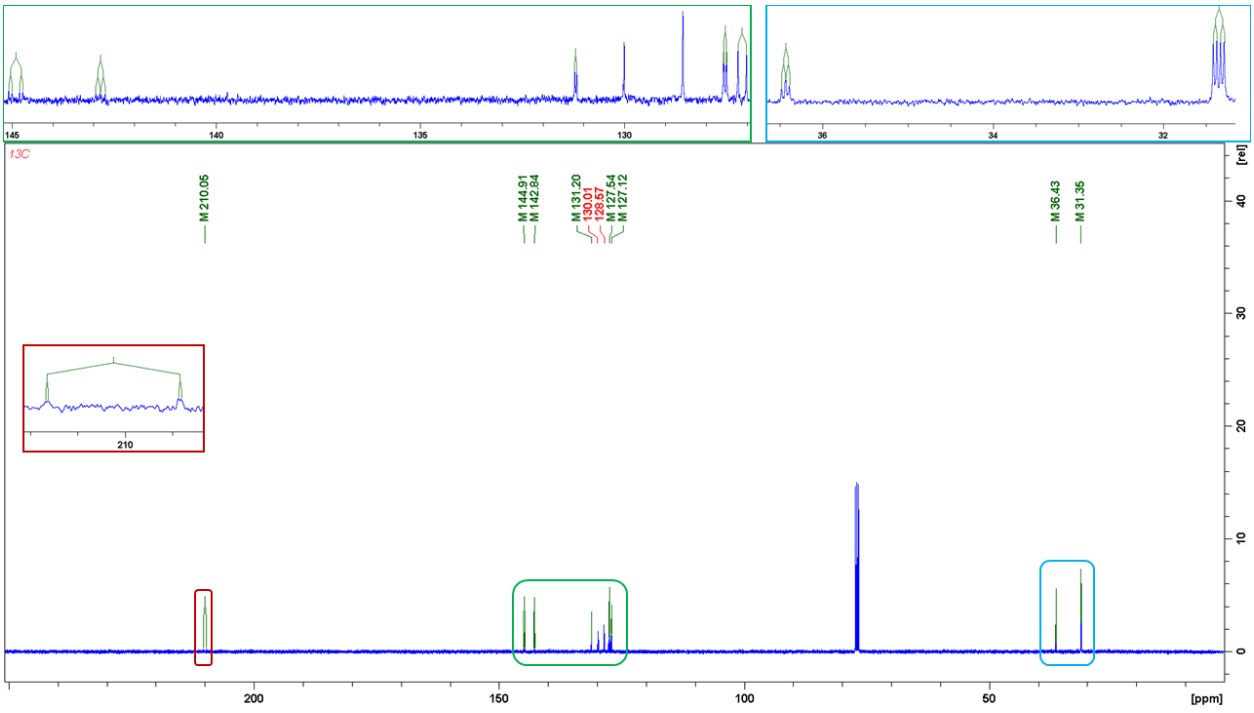

Figure S15. $^{13}C\{^{1}H\}$ NMR ($CDCl_3$, 100.6 MHz) spectrum of isolated $[Ph_2C{=}P\text{-}P(tBu_2)\text{-}AgCl]_2$ (**Ag1**).

- 210.06 ppm, dd, $J_{P\text{-}C}$ = 57.2 Hz, $J_{P\text{-}C}$ = 1.08 Hz, $[Ph_2\mathbf{C}{=}P\text{-}P(tBu_2)\text{-}AgCl]_2$;
- 144.91 ppm, dd, $J_{P\text{-}C}$ = 26.3 Hz, $J_{P\text{-}H}$ = 8.2 Hz, $[\mathbf{Ph}_2C{=}P\text{-}P(tBu_2)\text{-}AgCl]_2 - C_{Ar}$;
- 142.84 ppm, dd, $J_{P\text{-}C}$ = 13.7 Hz, $J_{P\text{-}H}$ = 10.2 Hz, $[\mathbf{Ph}_2C{=}P\text{-}P(tBu_2)\text{-}AgCl]_2 - C_{Ar}$;
- 131.20 ppm, d, $J_{P\text{-}C}$ = 5.2 Hz, $[\mathbf{Ph}_2C{=}P\text{-}P(tBu_2)\text{-}AgCl]_2 - C_{Ar}$;
- 130.01 ppm, s, $[\mathbf{Ph}_2C{=}P\text{-}P(tBu_2)\text{-}AgCl]_2 - C_{Ar}$;
- 128.57 ppm, s, $[\mathbf{Ph}_2C{=}P\text{-}P(tBu_2)\text{-}AgCl]_2 - C_{Ar}$;
- 127.54 ppm, d, $J_{P\text{-}C}$ = 7.0 Hz, $J_{P\text{-}C}$ = 1.6 Hz, $[\mathbf{Ph}_2C{=}P\text{-}P(tBu_2)\text{-}AgCl]_2 - C_{Ar}$;
- 127.12 ppm, d, $J_{P\text{-}C}$ = 20.4 Hz, $[\mathbf{Ph}_2C{=}P\text{-}P(tBu_2)\text{-}AgCl]_2 - C_{Ar}$;
- 36.43 ppm, dd, $J_{P\text{-}C}$ = 5.4 Hz, $J_{P\text{-}H}$ = 4.3 Hz, $[Ph_2C{=}P\text{-}P\{\mathbf{C}(CH_3)_2\}\text{-}AgCl]_2$;
- 30.93 ppm, dd, $J_{P\text{-}C}$ = 8.8 Hz, $J_{P\text{-}H}$ = 4.6 Hz, $[Ph_2C{=}P\text{-}P\{C(\mathbf{C}H_3)_2\}\text{-}AgCl]_2$;

2.2. Reaction of (p-MeO-Ph)$_2$C=P-PtBu$_2$ with AgCl.

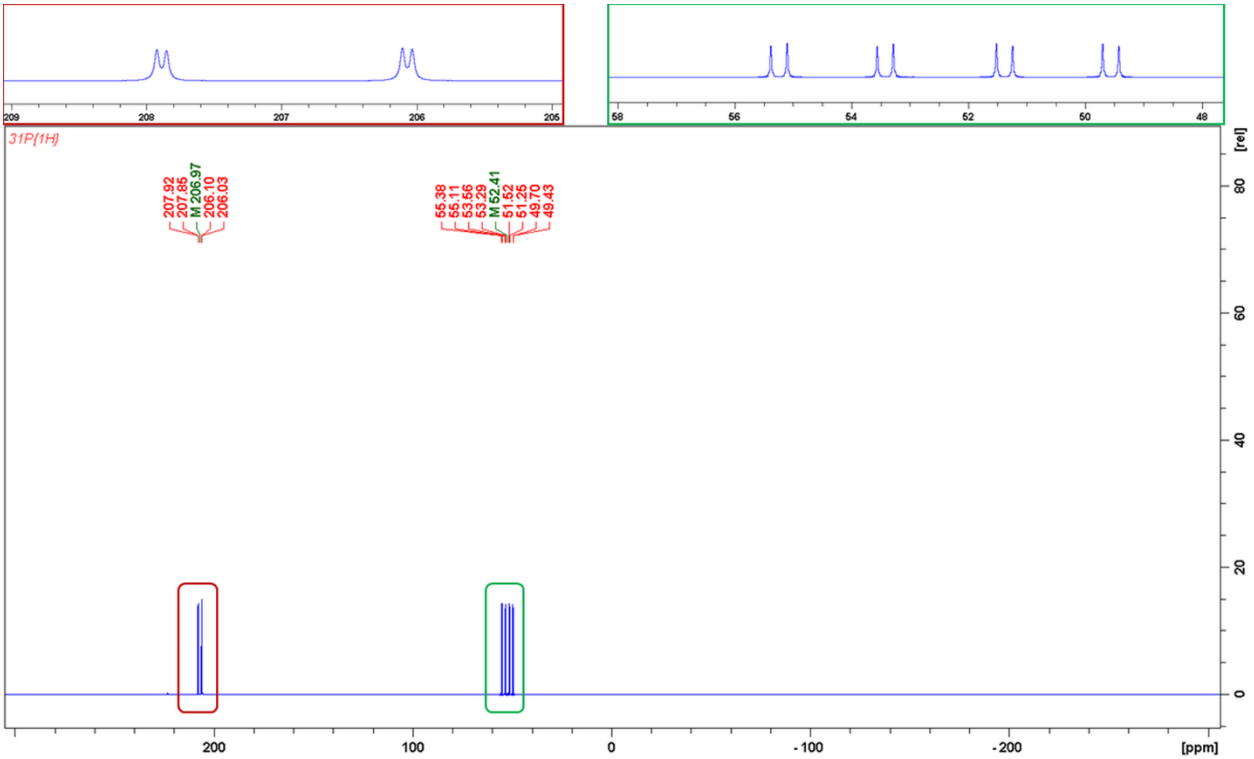

Figure S16. $^{31}P\{^{1}H\}$ NMR ($CDCl_3$, 162 MHz) spectrum of isolated [(p-MeO-Ph)$_2$C=P-P(tBu$_2$)-AgCl]$_2$ (**Ag2**).

- 206.97 ppm, dd, $J_{P\text{-}P}$ = 294.7 Hz, ^{2}J(Ag-^{31}P) = 11.7 Hz, [(p-MeO-Ph)$_2$C=**P**-P(tBu$_2$)-AgCl]$_2$, due to the low P-Ag coupling constant by two bonds and wide signals, only one P-Ag coupling constant is visible;
- 52.41 ppm, ddd, $J_{P\text{-}P}$ = 294.7 Hz, ^{1}J(^{107}Ag-^{31}P) = 590.5 Hz, ^{1}J(^{109}Ag-^{31}P) = 625.4 Hz, [(p-MeO-Ph)$_2$C=P-**P**(tBu$_2$)-AgCl]$_2$;

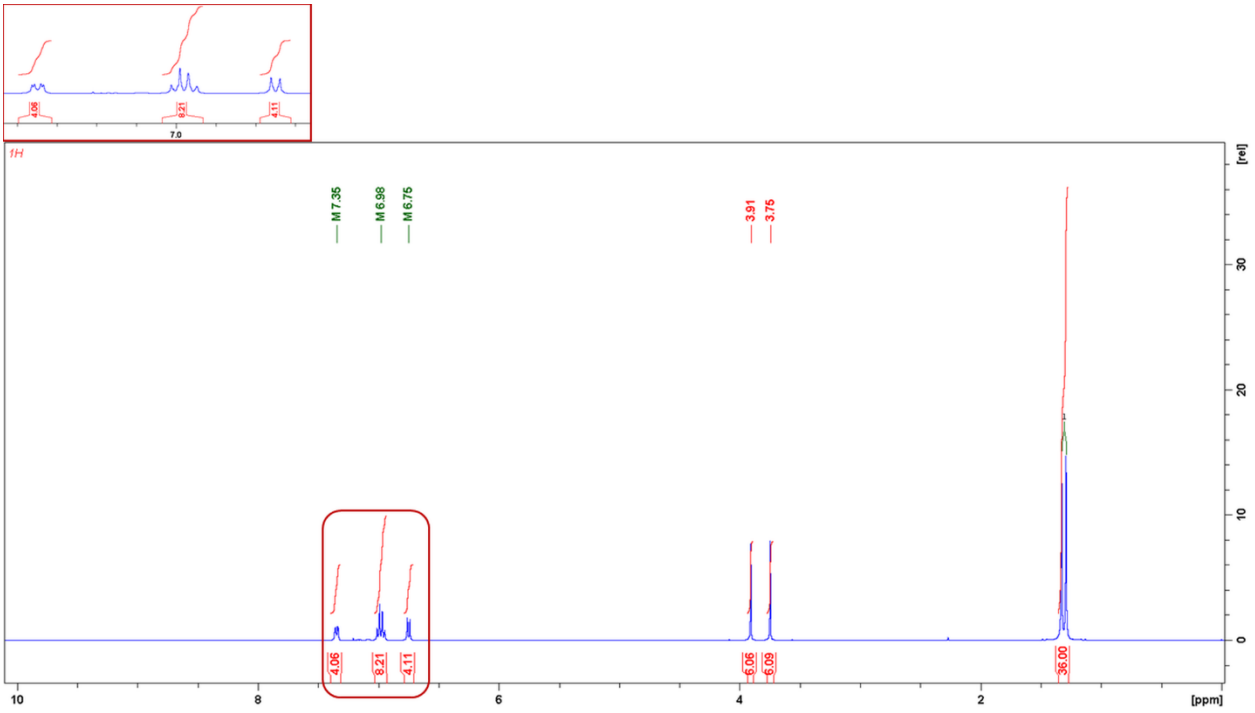

Figure S17. ^{1}H NMR ($CDCl_3$, 400 Hz) spectrum of isolated [(*p*-MeO-Ph)$_2$C=P-P(*t*Bu$_2$)-AgCl]$_2$ (**Ag2**).

- 7.35 ppm, 6.98 ppm, 6.75 ppm, 16H, [(*p*-MeO-**Ph**)$_2$C=P-P(*t*Bu$_2$)-AgCl]$_2$ – H_{Ar};
- 3.91 ppm, s, 6H, [(*p*-**Me**O-Ph)$_2$C=P-P(*t*Bu$_2$)-AgCl]$_2$;
- 3.75 ppm, s, 6H, [(*p*-**Me**O-Ph)$_2$C=P-P(*t*Bu$_2$)-AgCl]$_2$;
- 1.31 ppm, d, $J_{P\text{-}H}$ = 14.9 Hz, 36 H, [(*p*-MeO-Ph)$_2$C=P-P(*t*Bu$_2$)-AgCl]$_2$;

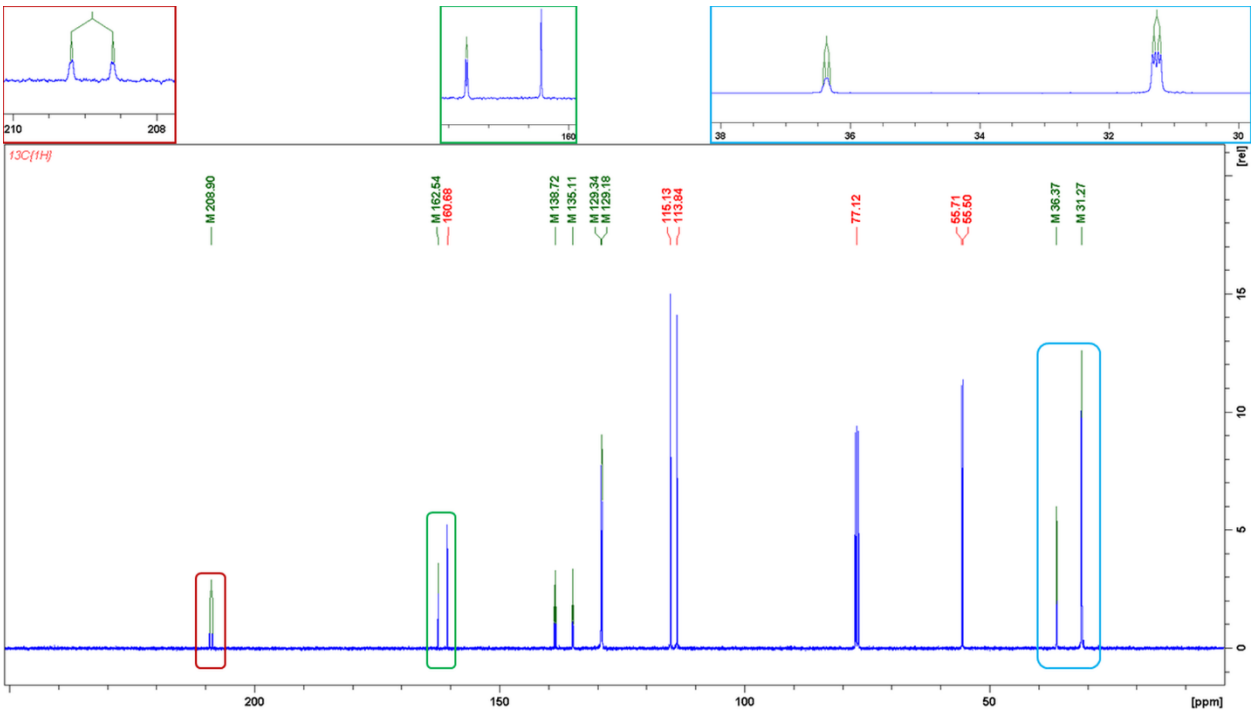

Figure S18. $^{13}C\{^{1}H\}$ NMR ($CDCl_3$, 100.6 Hz) spectrum of isolated [(*p*-MeO-Ph)$_2$C=P-P(*t*Bu$_2$)-AgCl]$_2$ (**Ag2**).

- 208.90 ppm, dd, $J_{P\text{-}C}$ = 58.2, $J_{P\text{-}C}$ = 3.0 Hz, [(*p*-MeO-Ph)$_2$**C**=P-P(*t*Bu$_2$)-AgCl]$_2$;
- 162.54 ppm, d, $J_{P\text{-}C}$ = 4.7 Hz, [(*p*-MeO-**Ph**)$_2$C=P-P(*t*Bu$_2$)-AgCl]$_2$ – C_{Ar};
- 160.68 ppm, s, [(*p*-MeO-**Ph**)$_2$C=P-P(*t*Bu$_2$)-AgCl]$_2$ – C_{Ar};
- 138.72 ppm, dd, $J_{P\text{-}C}$ = 27.5, $J_{P\text{-}C}$ = 8.3 Hz, [(*p*-MeO-**Ph**)$_2$C=P-P(*t*Bu$_2$)-AgCl]$_2$ – C_{Ar};
- 135.11 ppm, dd, $J_{P\text{-}C}$ = 13.3, $J_{P\text{-}C}$ = 9.9 Hz, [(*p*-MeO-**Ph**)$_2$C=P-P(*t*Bu$_2$)-AgCl]$_2$ – C_{Ar};
- 129.34 ppm, dd, $J_{P\text{-}C}$ = 5.8, $J_{P\text{-}C}$ = 1.5 Hz, [(*p*-MeO-**Ph**)$_2$C=P-P(*t*Bu$_2$)-AgCl]$_2$ – C_{Ar};
- 129.18 ppm, d, $J_{P\text{-}C}$ = 20.7 Hz, [(*p*-MeO-**Ph**)$_2$C=P-P(*t*Bu$_2$)-AgCl]$_2$ – C_{Ar};
- 115.13 ppm, s, [(*p*-MeO-**Ph**)$_2$C=P-P(*t*Bu$_2$)-AgCl]$_2$ – C_{Ar};
- 113.84 ppm, s, [(*p*-MeO-**Ph**)$_2$C=P-P(*t*Bu$_2$)-AgCl]$_2$ – C_{Ar};
- 77.12 ppm, t, $CDCl_3$;
- 55.71 ppm, s, [(*p*-**Me**O-Ph)$_2$C=P-P(*t*Bu$_2$)-AgCl]$_2$;
- 55.50 ppm, s, [(*p*-**Me**O-Ph)$_2$C=P-P(*t*Bu$_2$)-AgCl]$_2$;
- 36.37 ppm, dd, $J_{P\text{-}C}$ = 7.5 Hz, $J_{P\text{-}C}$ = 3.3 Hz, [(*p*-MeO-Ph)$_2$C=P-P{**C**(CH$_3$)$_2$}-AgCl]$_2$;
- 31.27 ppm, dd, $J_{P\text{-}C}$ = 8.5 Hz, $J_{P\text{-}C}$ = 3.9 Hz, [(*p*-MeO-Ph)$_2$C=P-P{C(**C**H$_3$)$_2$}-AgCl]$_2$;

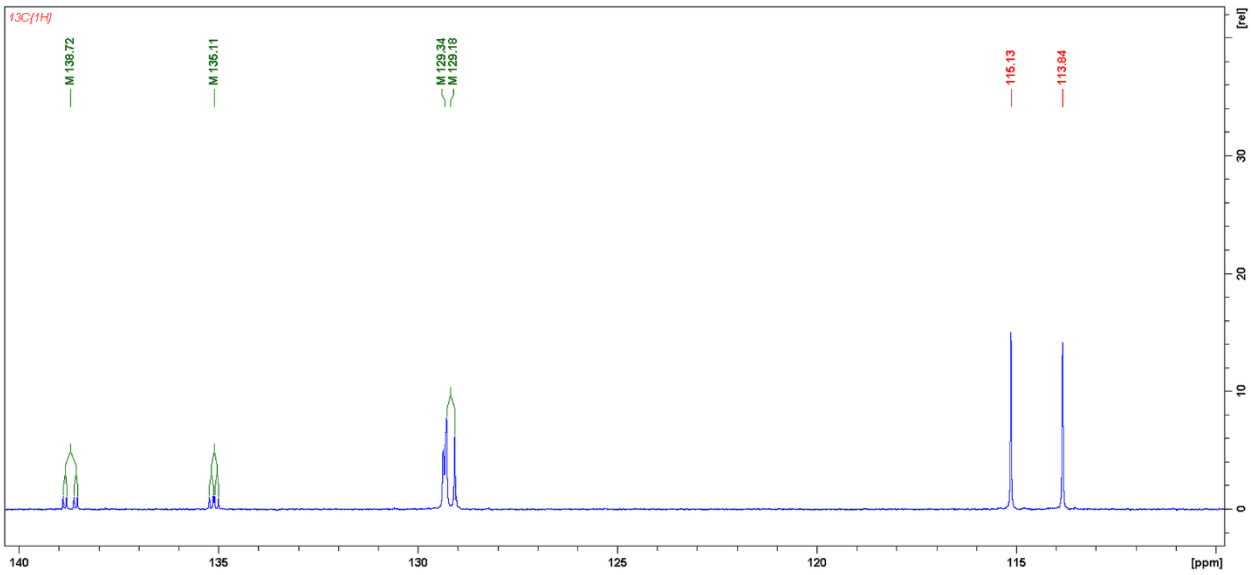

Figure S19. $^{13}C\{^{1}H\}$ NMR ($CDCl_3$, 100.6 Hz) spectrum of isolated [(*p*-MeO-Ph)$_2$C=P-P(*t*Bu$_2$)-AgCl]$_2$ (**Ag2**) in the range from 140 ppm to 110 ppm.

3. Reaction of phosphanylphosphaalkenes with (tht)AuCl.

3.1 Reaction of Ph_2C=P-P*t*Bu_2 with (tht)AuCl.

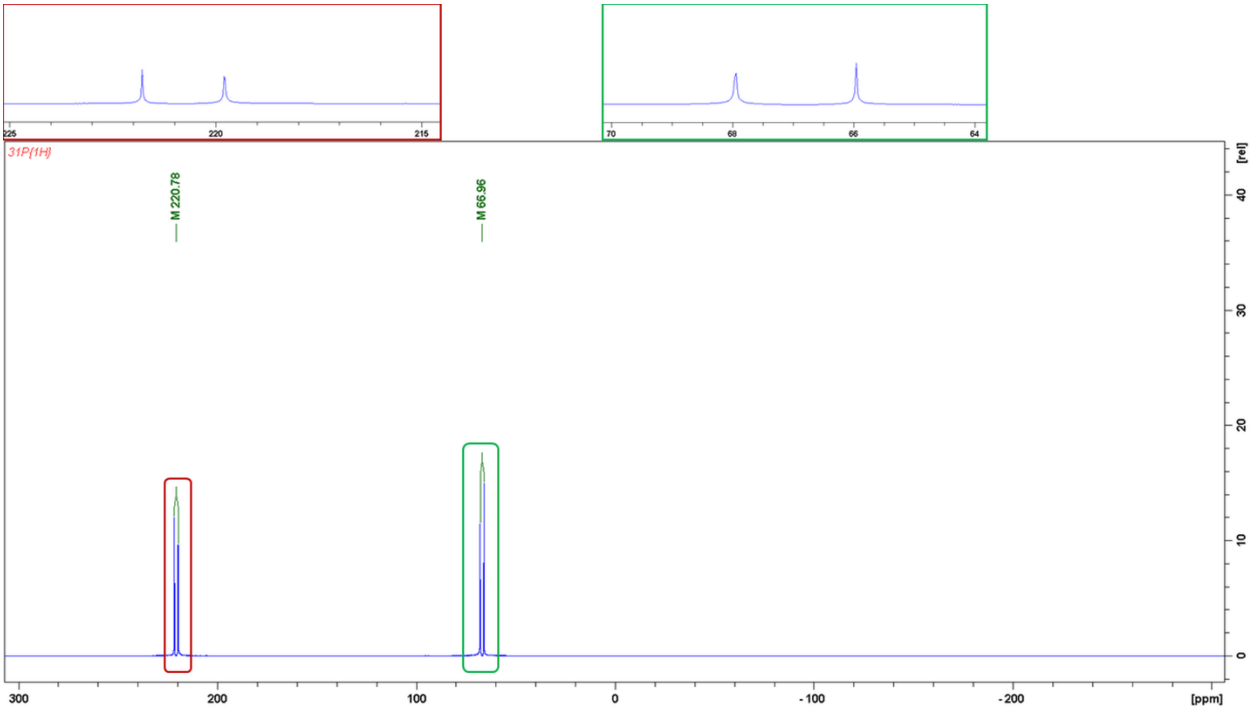

Figure S20. $^{31}P\{^{1}H\}$ NMR (C_6D_6, 162 MHz) spectrum of isolated [Ph_2C=P-P(*t*Bu_2)-AuCl] (**Au1**).

- 200.78 ppm, d, $J_{P\text{-}P}$ = 321.2 Hz, [Ph_2C=**P**-P(*t*Bu_2)-AuCl];
- 66.96 ppm, d, $J_{P\text{-}P}$ = 321.2 Hz, [Ph_2C=P-**P**(*t*Bu_2)-AuCl];

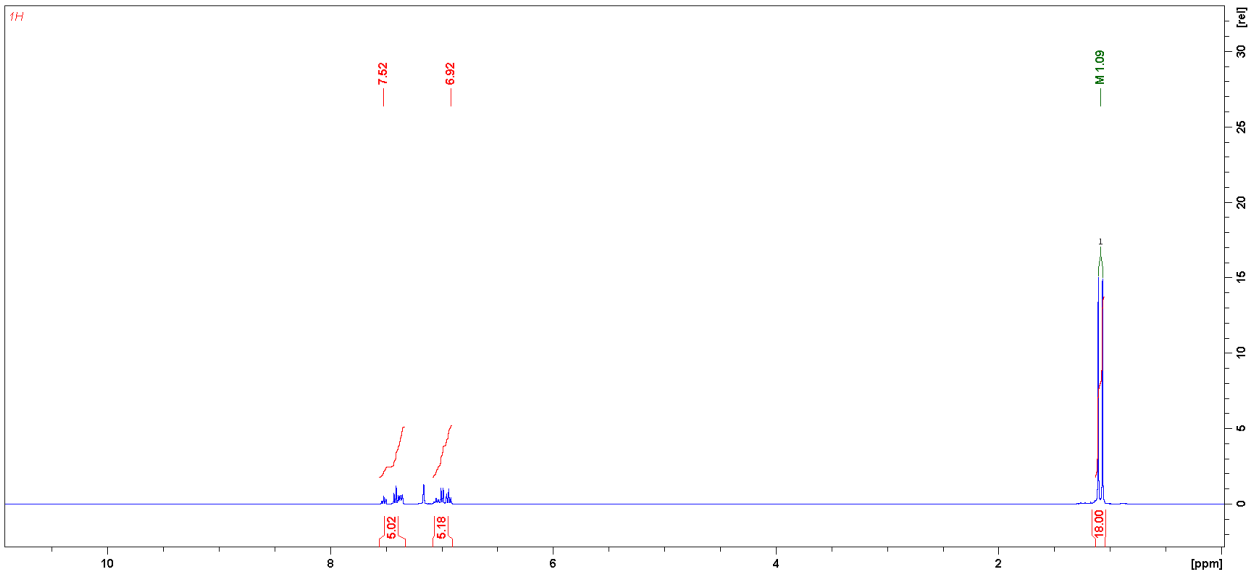

Figure S21. ^{1}H NMR (C_6D_6, 400 MHz) spectrum of [Ph_2C=P-P(tBu$_2$)-AuCl] (**Au1**).

- from 7.52 ppm to 6.92 ppm, 10H, [**Ph**$_2$C=P-P(tBu$_2$)-AuCl] – H_{Ar};
- 1.09 ppm, d, $J_{P\text{-}H}$ = 15.4 Hz, 18H [Ph_2C=P-P(***t*Bu$_2$**)-AuCl];

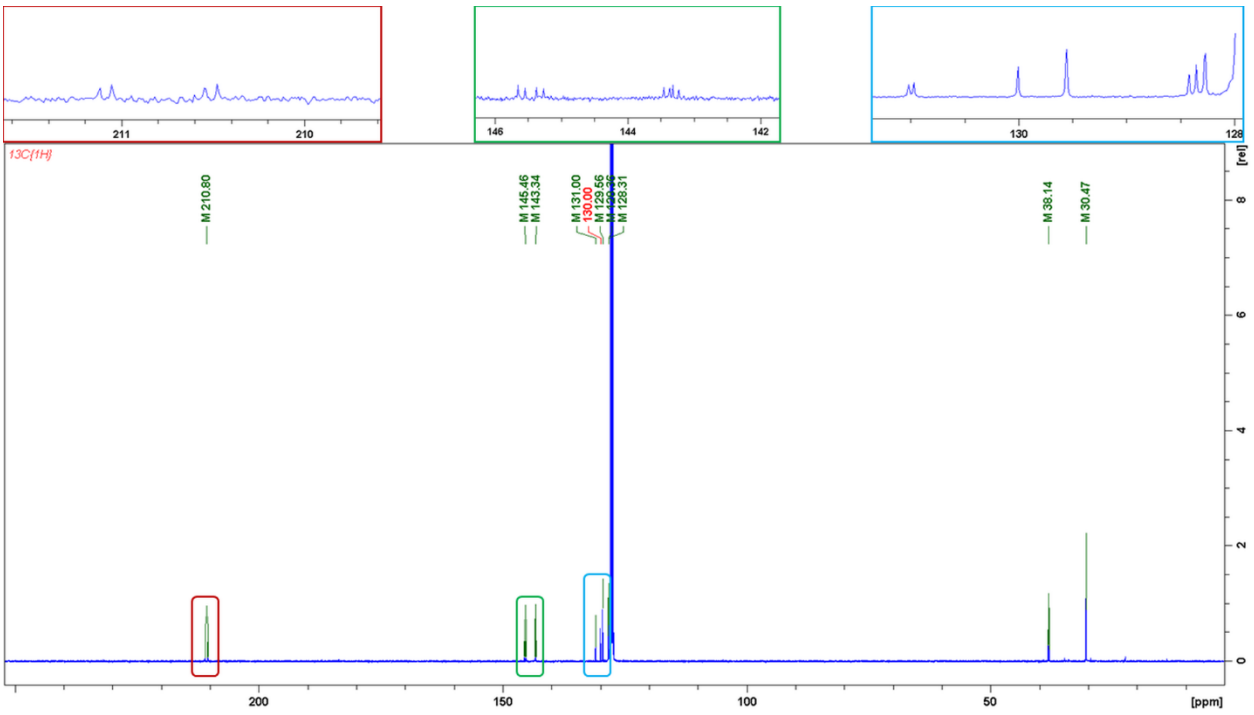

Figure S22. $^{13}C\{^{1}H\}$ NMR (C_6D_6, 100.6 MHz) spectrum of isolated [Ph_2C=P-P(tBu$_2$)-AuCl] (**Au1**).

- 210.80 ppm, dd, $J_{P\text{-}C}$ = 58.1 Hz, $J_{P\text{-}C}$ = 6.4 Hz, [Ph_2**C**=P-P(tBu$_2$)-AuCl];
- 145.46 ppm, dd, $J_{P\text{-}C}$ = 28.2 Hz, $J_{P\text{-}H}$ = 10.9 Hz, [**Ph**$_2$C=P-P(tBu$_2$)-AuCl – C_{Ar};
- 143.34 ppm, dd, $J_{P\text{-}C}$ = 13.6 Hz, $J_{P\text{-}H}$ = 10.9 Hz, [**Ph**$_2$C=P-P(tBu$_2$)-AuCl – C_{Ar};
- 131.00 ppm, d, $J_{P\text{-}C}$ = 4.5 Hz,[**Ph**$_2$C=P-P(tBu$_2$)-AuCl] – C_{Ar};
- 130.00 ppm, s, [**Ph**$_2$C=P-P(tBu$_2$)-AuCl] – C_{Ar};
- 129.56 ppm, d, $J_{P\text{-}C}$ = 0.9 Hz, [**Ph**$_2$C=P-P(tBu$_2$)-AuCl] – C_{Ar};
- 128.36 ppm, d, $J_{P\text{-}C}$ = 14.5 Hz, [**Ph**$_2$C=P-P(tBu$_2$)-AuCl] – C_{Ar};
- 128.31 ppm, d, $J_{P\text{-}C}$ = 8.2 Hz, [**Ph**$_2$C=P-P(tBu$_2$)-AuCl] – C_{Ar};
- 38.14 ppm, dd, $J_{P\text{-}C}$ = 19.1 Hz, $J_{P\text{-}H}$ = 5.4 Hz, [Ph_2C=P-P{**C**(CH_3)$_2$}-AuCl];
- 30.47 ppm, dd, $J_{P\text{-}C}$ = 5.4 Hz, $J_{P\text{-}H}$ = 4.5 Hz, [Ph_2C=P-P{C(**C**H_3)$_2$}-AuCl];

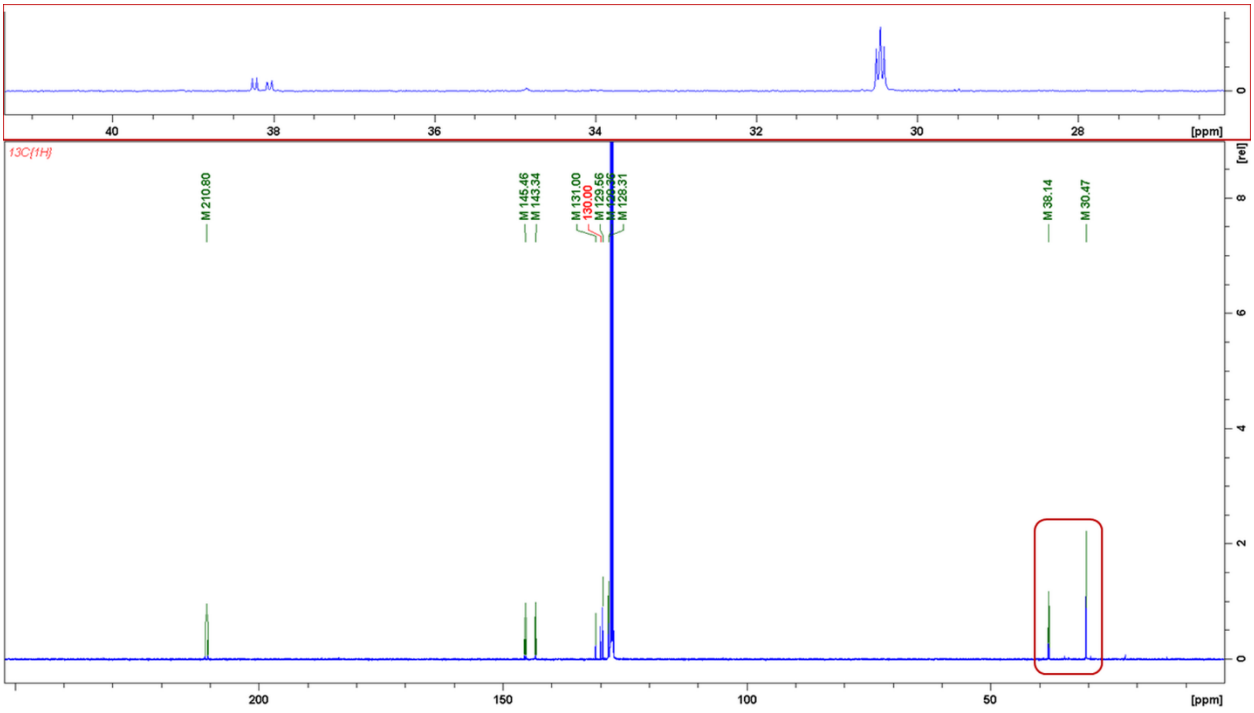

Figure S23. $^{13}C\{^{1}H\}$ NMR (C_6D_6, 100.6 MHz) spectrum of isolated [Ph_2C=P-P(tBu$_2$)-AuCl] (**Au1**) with additional presentation of range from 40 ppm to 25 ppm.

3.2. Reaction of (p-MeO-Ph)$_2$C=P-PtBu$_2$ with (tht)AuCl.

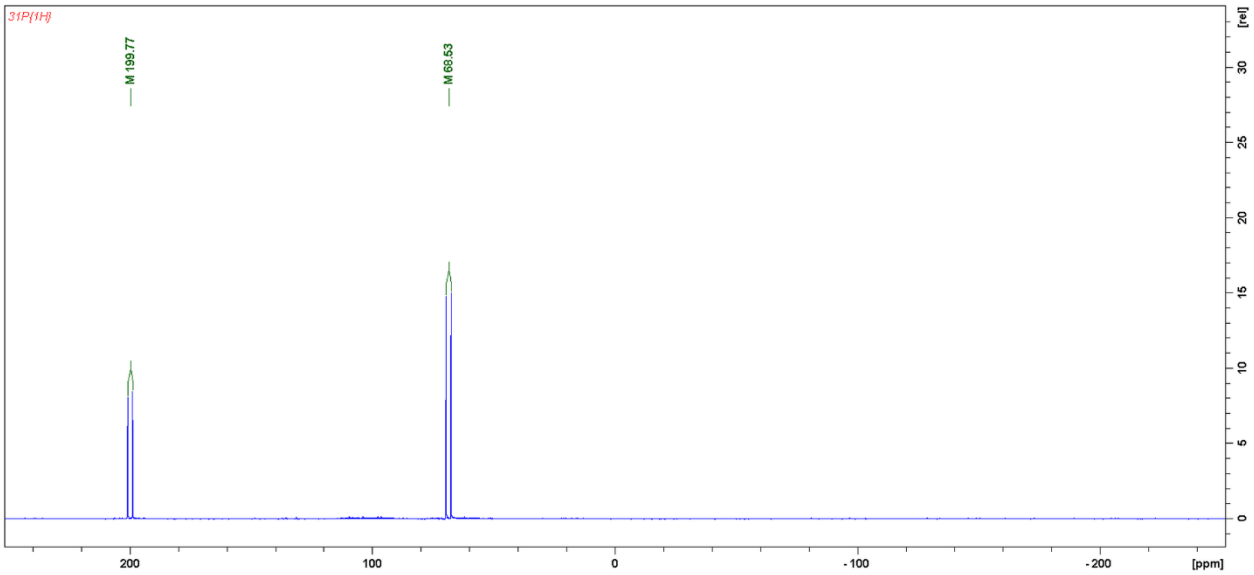

Figure S24. $^{31}P\{^{1}H\}$ NMR (C_6D_6, 162 MHz) spectrum of reaction mixture of (p-MeO-Ph)$_2$C=P-PtBu$_2$ with (tht)AuCl.

- 199.77 ppm, d, $J_{P\text{-}P}$ = 330.9 Hz, [(p-MeO-Ph)$_2$C=**P**-P(tBu$_2$)-AuCl];
- 68.53 ppm, d, $J_{P\text{-}P}$ = 330.9 Hz, [(p-MeO-Ph)$_2$C=P-**P**(tBu$_2$)-AuCl];

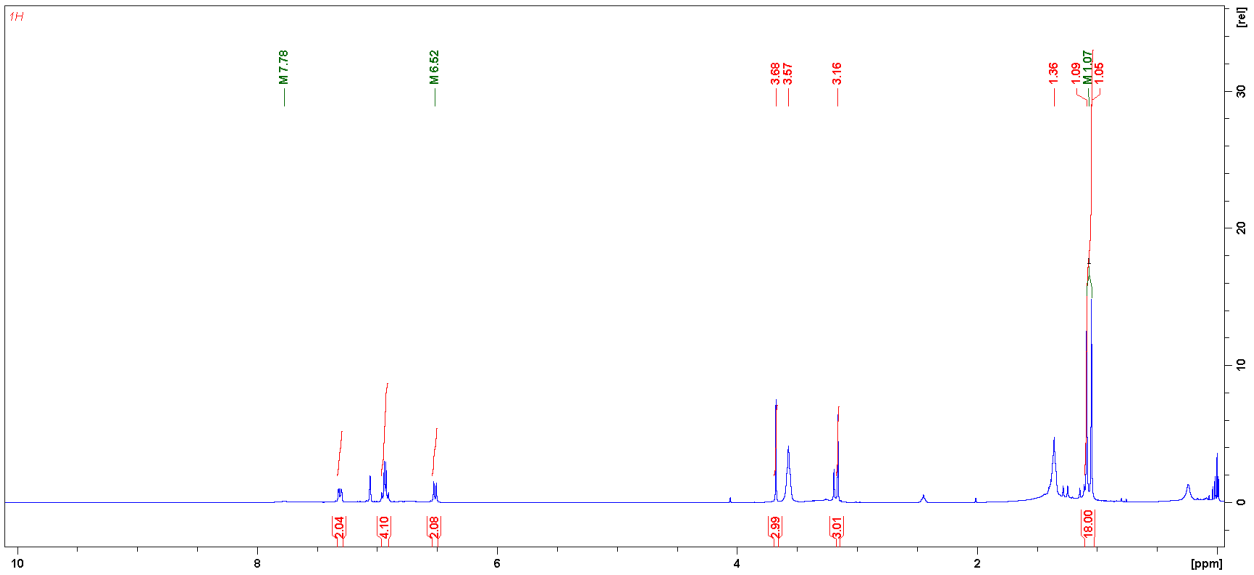

Figure S25. ^{1}H NMR (C_6D_6, 400 MHz) spectrum of reaction mixture of (p-MeO-Ph)$_2$C=P-PtBu$_2$ with (tht)AuCl integrated for the [(p-MeO-Ph)$_2$C=P-P(tBu$_2$)-AuCl] complex.

- from 7.78 ppm to 6.52 ppm, 8H, [(p-MeO-**Ph**)$_2$C=P-P(tBu$_2$)-AuCl] – H$_{Ar}$;
- 3.68 ppm, s, 3H, [(p-**Me**O-Ph)$_2$C=P-P(tBu$_2$)-AuCl];
- 3.16 ppm, s, 3H, [(p-**Me**O-Ph)$_2$C=P-P(tBu$_2$)-AuCl];
- 1.07 ppm, d, $J_{P\text{-}H}$ = 15.4 Hz, 18 H, [(p-MeO-Ph)$_2$C=P-P(***t*Bu$_2$**)-AuCl];
- 3.57 ppm and 1.36 ppm, THF protons;

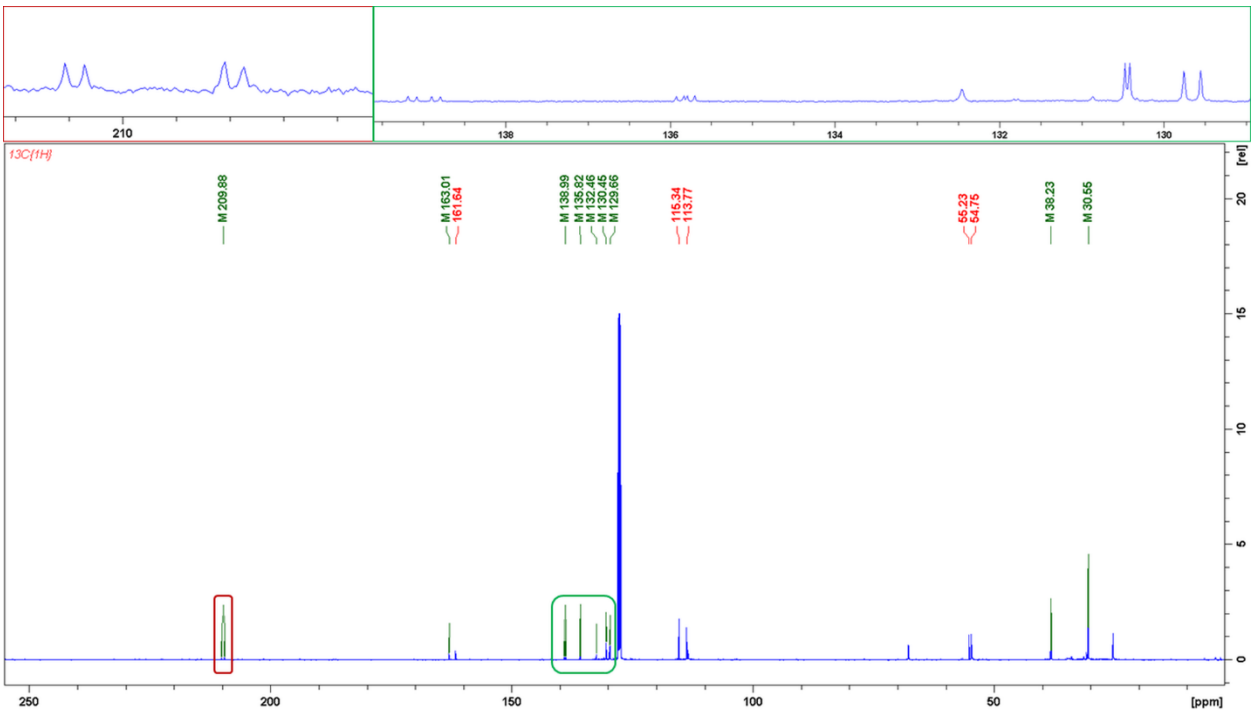

Figure S26. $^{13}C\{^{1}H\}$ NMR ($CDCl_3$, 100.6 Hz) spectrum of reaction mixture of (p-MeO-Ph)$_2$C=P-PtBu$_2$ with (tht)AuCl with marked shifts for the [(p-MeO-Ph)$_2$C=P-P(tBu$_2$)-AuCl] complex.

- 209.88 ppm, dd, $J_{P\text{-}C}$ = 59.4, $J_{P\text{-}C}$ = 7.3 Hz, [(p-MeO-Ph)$_2$**C**=P-P(tBu$_2$)-AuCl];
- 163.01 ppm, d, $J_{P\text{-}C}$ = 4.5 Hz, [(p-MeO-**Ph**)$_2$C=P-P(tBu$_2$)-AuCl] – C_{Ar};
- 161.64 ppm, s, [(p-MeO-**Ph**)$_2$C=P-P(tBu$_2$)-AuCl] – C_{Ar};
- 138.99 ppm, dd, $J_{P\text{-}C}$ = 28.6, $J_{P\text{-}C}$ = 10.4 Hz, [(p-MeO-**Ph**)$_2$C=P-P(tBu$_2$)-AuCl] – C_{Ar};
- 135.82 ppm, dd, $J_{P\text{-}C}$ = 13.62, $J_{P\text{-}C}$ = 9.1 Hz, [(p-MeO-**Ph**)$_2$C=P-P(tBu$_2$)-AuCl] – C_{Ar};
- 132.45 ppm, d, $J_{P\text{-}C}$ = 0.9 Hz, [(p-MeO-**Ph**)$_2$C=P-P(tBu$_2$)-AuCl] – C_{Ar};
- 130.45 ppm, d, $J_{P\text{-}C}$ = 5.4 Hz, [(p-MeO-**Ph**)$_2$C=P-P(tBu$_2$)-AuCl] – C_{Ar};
- 115.34 ppm, s, [(p-MeO-**Ph**)$_2$C=P-P(tBu$_2$)-AuCl] – C_{Ar};
- 113.77 ppm, s, [(p-MeO-**Ph**)$_2$C=P-P(tBu$_2$)-AuCl] – C_{Ar};
- 55.23 ppm, s, [(p-**Me**O-Ph)$_2$C=P-P(tBu$_2$)-AuCl];
- 54.75 ppm, s, [(p-**Me**O-Ph)$_2$C=P-P(tBu$_2$)-AuCl];
- 38.23 ppm, dd, $J_{P\text{-}C}$ = 18.2 Hz, $J_{P\text{-}C}$ = 5.4 Hz, [(p-MeO-Ph)$_2$C=P-P{**C**(CH$_3$)$_2$}-AuCl];
- 30.55 ppm, dd, $J_{P\text{-}C}$ = 5.4 Hz, $J_{P\text{-}C}$ = 4.5 Hz, [(p-MeO-Ph)$_2$C=P-P{**C**(CH$_3$)$_2$}-AuCl];

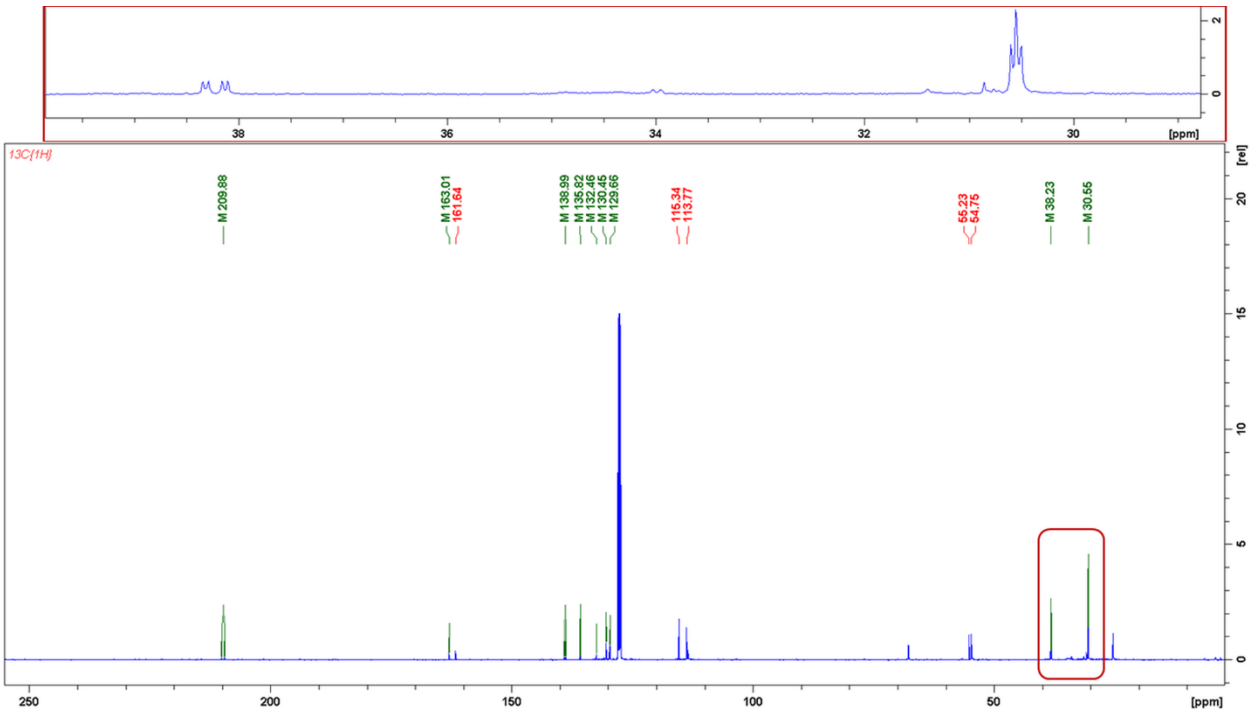

Figure S27. $^{13}C\{^{1}H\}$ NMR ($CDCl_3$, 100.6 Hz) spectrum of reaction mixture of (p-MeO-Ph)$_2$C=P-PtBu$_2$ with (tht)AuCl with marked shifts for the [(p-MeO-Ph)$_2$C=P-P(tBu$_2$)-AuCl] complex.

PART D. DFT RESULTS

All calculations presented in the paper were performed using the Gaussian 09 program package.[3] Molecular geometries of C=P and C=P-P ligands were optimized using density functional theory at the B3PW91 functional with 6-311++G(3df,2p) basis set.[4, 5] The B3PW91/6-311++G(3df,2p) method has been chosen to compare the obtained results with the theoretical study presented in the previous work on the electronic properties of C=P ligands.[6] Molecular geometries were energy-optimized, and the most stable (the lowest energy) conformer was identified during the potential energy surface scanning. The nature of the final gas-phase geometries as local minima (no imaginary frequencies) on the potential energy surface was then validated by harmonic frequency calculations at the same level of theory. NBO analysis was performed for optimized gas-phase structures at the same B3PW91/6-311++G(3df,2p) level of theory by applying the NBO 3.1 module built-in Gaussian 09.[7]

The NBO (Natural Bond Orbitals) analysis, including Wiberg bond orders and second-order perturbative estimates of donor-acceptor interactions in the NBO basis calculations discussed in this paper, were performed on non-optimized X-ray structures of **Cu1**, **Cu2**, **Ag1** and **Ag2** using density functional theory at the WB97XD[8, 9] level of theory with LANL2DZ basis set for Ag and Cu atoms and Def2TZVP[10, 11]8,9 for non-metals by applying implemented in Gaussian091 package version of NBO 3.1 program.[7]

Table 3. NBO analysis of P-lone pairs together with NPA charges calculated at B3PW91/6-311++G(3df,2p) level of theory.

Compound	s- and p-orbital contribution to lone pairs (LP)				NPA charges		
	$LP_{C=P}$		LP_{PtBu2}		C=P-P*t*Bu$_2$ /C=P*t*Bu	C=P-P*t*Bu$_2$ /C=P*t*Bu	C=P-P*t*Bu$_2$
	s-orbital [%]	p-orbital [%]	s-orbital [%]	p-orbital [%]			
Ph_2C=P-P*t*Bu$_2$	65.51	34.40	54.38	45.53	-0.358	0.341	0.576
[(*p*-MeO-Ph)$_2$C=P-P*t*Bu$_2$	65.44	34.46	54.16	45.74	-0.435	0.310	0.573
Ph_2C=P*t*Bu	62.98	36.95	-	-	-0.410	0.717	-
(*p*-MeO-Ph)$_2$C=P*t*Bu	63.05	36.88	-	-	-0.434	0.68	-

Optimized structures and Cartesian coordinates
In all structures the hydrogen atoms (except those of P=C(H) moiety) were omitted for clarity.

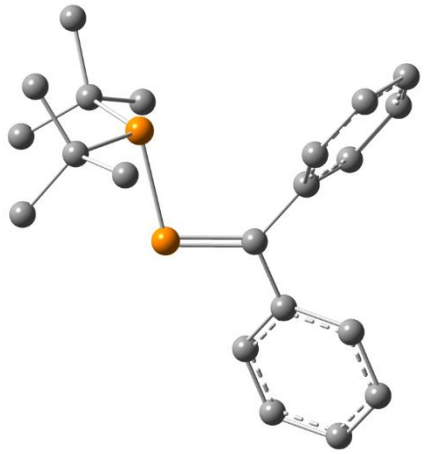

Figure S28. Optimized structure of Ph_2C=P-P*t*Bu$_2$.

C	-1.25796200	-0.17099000	-0.12880800
C	-2.56200200	-0.86630900	-0.07589200
C	-2.72205400	-2.08929000	0.58780700
H	-1.88174500	-2.50719400	1.12806500
C	-3.93922200	-2.75126100	0.57897400
H	-4.04106100	-3.69197700	1.10670800
C	-5.02846200	-2.20466900	-0.08673100
H	-5.98129100	-2.72009300	-0.08883200
C	-4.89157700	-0.98500500	-0.73781600
H	-5.73617300	-0.54890600	-1.25776700

C	-3.67732800	-0.31899800	-0.72496100
H	-3.57882800	0.62918300	-1.23819700
C	-1.31272400	1.30524900	-0.09956900
C	-0.74138000	2.08476200	-1.10657500
H	-0.24573900	1.59520700	-1.93401100
C	-0.82309700	3.46842300	-1.06416800
H	-0.38325300	4.05544100	-1.86146500
C	-1.46085100	4.09970800	-0.00524500
H	-1.51691800	5.18097500	0.03100800
C	-2.03414400	3.33616500	1.00382300
H	-2.53692000	3.81937900	1.83309800
C	-1.97565200	1.95251900	0.94832500
H	-2.43687900	1.36056900	1.72975800
C	2.96133500	-0.59306600	-1.42620600
C	3.00682800	-2.12020000	-1.50703000
H	3.61826700	-2.41752100	-2.36606900
H	2.01513800	-2.55269800	-1.64719300
H	3.44717800	-2.57277000	-0.62057600
C	2.35812600	-0.05578500	-2.73200900
H	2.34950600	1.03582700	-2.75102800
H	1.33395400	-0.40809500	-2.87845800
H	2.95159600	-0.40623900	-3.58224400
C	4.38642400	-0.04906700	-1.29546700
H	4.91544000	-0.48964000	-0.44984100
H	4.39894300	1.03700400	-1.18052900
H	4.95486000	-0.29662700	-2.19779200
C	2.50116100	-0.25361500	1.67576900
C	1.34011000	0.07555600	2.62207400
H	1.69072200	0.01787300	3.65727900
H	0.51092900	-0.62467600	2.51036900
H	0.95512700	1.08347600	2.45325300
C	3.65239900	0.70570100	2.00470000
H	3.94655900	0.57322400	3.05116000
H	3.35210400	1.74635500	1.86931500
H	4.53493500	0.52751300	1.39189000
C	2.94529100	-1.69593100	1.90622000
H	3.85002000	-1.93876500	1.34847700
H	2.16972600	-2.41242100	1.63010400
H	3.17143800	-1.84455800	2.96785400
P	0.11874000	-1.16421800	-0.23986900
P	1.86932900	0.19933600	-0.07197300

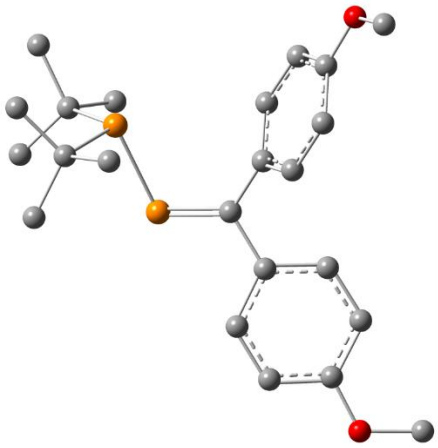

Figure S29. Optimized structure of (p-(MeO)-Ph)$_2$C=P-PtBu$_2$.

C	0.66074400	-0.30945300	-0.14830500
C	2.04574600	-0.79952400	-0.01123500
C	2.36283900	-1.95705800	0.71766700
H	1.57467400	-2.46962000	1.25503100
C	3.65263800	-2.43841100	0.78373100
H	3.88942000	-3.32368100	1.36024600
C	4.68589200	-1.77425600	0.12026100
C	4.40165400	-0.61445700	-0.59808200
H	5.18083700	-0.07797500	-1.12139300
C	3.10037000	-0.13872800	-0.64863800
H	2.89390900	0.75841500	-1.21853400
C	6.99985900	-1.67766300	-0.39906200
H	6.85854500	-1.64448700	-1.48341600
H	7.88158700	-2.27239400	-0.17166700
H	7.14471200	-0.66085400	-0.02199500
C	0.49462800	1.15364900	-0.21779100
C	1.08442200	1.97462200	0.74380000
H	1.66074600	1.52376600	1.54287900
C	0.93791600	3.35460900	0.71860100
H	1.39470500	3.94964700	1.49708500
C	0.21325100	3.95006500	-0.31113100
C	-0.35797700	3.14793500	-1.29974900
H	-0.90420200	3.62379900	-2.10421300
C	-0.22709100	1.77618200	-1.24341100
H	-0.67084300	1.16600700	-2.01816300
C	0.57876800	6.13817400	0.53224100
H	0.17749000	5.92787300	1.52826200
H	0.30285000	7.14957500	0.24239100
H	1.66973100	6.05694900	0.55840400
C	-3.49142600	-1.51398000	-1.34608000
C	-2.75084600	-1.39311600	-2.68458800

H	-3.34195100	-1.87231500	-3.47143000
H	-1.77319400	-1.87896700	-2.65980200
H	-2.60451800	-0.34836800	-2.96879900
C	-4.87107400	-0.86727700	-1.52538500
H	-5.40648200	-1.37042100	-2.33735900
H	-4.78314700	0.18950300	-1.78501300
H	-5.48823000	-0.94282400	-0.63134500
C	-3.65567500	-2.99181300	-0.99633200
H	-4.27598900	-3.13328600	-0.11086700
H	-2.69547500	-3.48102500	-0.82468900
H	-4.15040800	-3.51316100	-1.82333400
C	-2.97186300	-0.82450300	1.68664000
C	-2.63751300	-2.21685600	2.22221400
H	-1.57165400	-2.43681100	2.14004600
H	-3.18195400	-3.00647600	1.70727300
H	-2.90332800	-2.27014000	3.28376900
C	-2.17838100	0.21289300	2.49263900
H	-2.41711000	0.10981200	3.55613600
H	-2.42001700	1.23152400	2.18460900
H	-1.10185500	0.07352600	2.37692400
C	-4.46454800	-0.54769800	1.87872200
H	-4.69437100	-0.52594800	2.94916000
H	-5.08599600	-1.32348000	1.43038200
H	-4.75731400	0.41594300	1.45612400
O	5.91864500	-2.31695300	0.24285500
O	0.02012600	5.28409000	-0.44044700
P	-0.54713300	-1.51056500	-0.24285600
P	-2.49188900	-0.43751600	-0.12623300

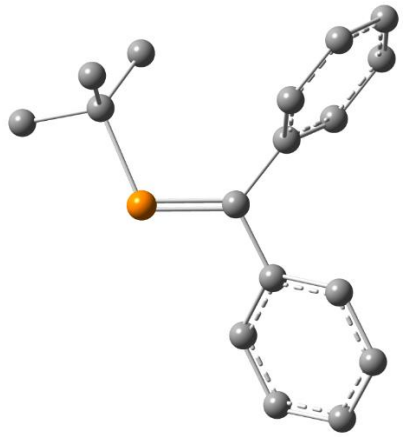

Figure S30. Optimized structure of $Ph_2C{=}PtBu$.

C	-0.28722000	-0.30323800	-0.05672700
C	-1.76342900	-0.42077100	-0.04322000
C	-2.41382100	-1.51063700	0.54972100
H	-1.82264600	-2.25918400	1.06226000
C	-3.79393100	-1.62687200	0.50861100
H	-4.27312800	-2.47713800	0.97915500
C	-4.56175100	-0.64984100	-0.11121300
H	-5.64125900	-0.73687100	-0.13510000
C	-3.93484200	0.44896600	-0.68482900
H	-4.52404800	1.22089400	-1.16549300
C	-2.55510900	0.56636200	-0.64551600
H	-2.07793900	1.42536600	-1.10022600
C	0.24219900	1.07740300	0.02682600
C	0.88415000	1.67780800	-1.05669600
H	0.99011300	1.12163300	-1.97958800
C	1.35985000	2.97978800	-0.96863700
H	1.85075900	3.43025800	-1.82315700
C	1.20380900	3.70204800	0.20543700
H	1.58042000	4.71513000	0.27698200
C	0.55008600	3.12083500	1.28571700
H	0.41629500	3.68015200	2.20403600
C	0.06098100	1.82776100	1.19242600
H	-0.45588800	1.38143900	2.03346400
P	0.57149600	-1.75087200	-0.21781300
C	2.43524600	-1.51265700	0.00274100
C	3.09375000	-1.13730000	-1.32847600
C	2.84517300	-0.53968300	1.10592100
C	2.89956800	-2.92649200	0.39335800
H	2.77279700	-1.79624600	-2.13898300
H	2.86773600	-0.11110800	-1.61444400

H	4.18166800	-1.22822500	-1.24038100
H	2.35233200	-0.77474000	2.05152400
H	3.92588300	-0.61153800	1.26966500
H	2.61712100	0.49378800	0.85375900
H	3.98808000	-2.93880600	0.50129300
H	2.46418200	-3.24656500	1.34275600
H	2.62683600	-3.66603800	-0.36299200

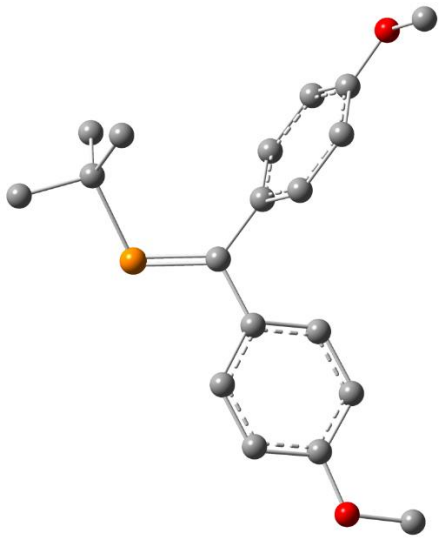

Figure S31. Optimized structure of (*p*-(MeO)-Ph)$_2$C=P*t*Bu.

C	0.11281300	0.81143200	0.05702100
C	1.53755900	0.43351200	-0.03571400
C	2.48395800	1.22884100	-0.70254500
H	2.14879200	2.11947000	-1.21937800
C	3.81934000	0.88933500	-0.73454400
H	4.53845600	1.50375100	-1.26145600
C	4.26524300	-0.27475400	-0.10615400
C	3.34476100	-1.09355400	0.54359400
H	3.65798400	-2.00441300	1.03463600
C	2.00401800	-0.73856500	0.56632700
H	1.30405800	-1.38253400	1.08391200
C	6.08887200	-1.70273500	0.41037000
H	5.91577100	-1.69947600	1.49074200
H	7.15976800	-1.71133300	0.22028500
H	5.63926000	-2.60055700	-0.02452000
C	-0.84555500	-0.31408500	0.10653800
C	-0.96322800	-1.19325800	-0.96889400
H	-0.35149500	-1.03617200	-1.84928700
C	-1.86079600	-2.25184900	-0.95186900
H	-1.93521400	-2.89574100	-1.81723200
C	-2.64612700	-2.47380400	0.17777300
C	-2.51368300	-1.62796600	1.27819700
H	-3.11037800	-1.82358900	2.16026800
C	-1.62958000	-0.56625600	1.23642200
H	-1.52170300	0.07247400	2.10392900
C	-3.71081300	-4.36581400	-0.78218100
H	-4.05361000	-3.84196800	-1.67966000

H	-4.46974600	-5.08187800	-0.47512900
H	-2.78334800	-4.90058200	-1.00864800
O	5.59136200	-0.53081900	-0.19569800
O	-3.54512500	-3.47957900	0.30186400
P	-0.21658000	2.47171000	0.15086900
C	-2.06338500	2.85282200	-0.02679900
C	-2.81494600	1.99348500	-1.04084700
C	-2.76339500	2.82533500	1.33526300
C	-2.04504100	4.30629500	-0.53140100
H	-2.30671700	1.97879300	-2.00720800
H	-2.93328800	0.96504600	-0.70596100
H	-3.81599800	2.40972200	-1.19907600
H	-2.21088600	3.39688700	2.08500400
H	-3.76034300	3.27092200	1.24842000
H	-2.88584700	1.80847700	1.70529800
H	-3.07057900	4.67504100	-0.62840300
H	-1.51218000	4.96678000	0.15655100
H	-1.56404500	4.38791700	-1.50879200

PART E. EDS analysis

The topography analysis was carried out using FEI Quanta FEG 250 scanning electron microscope (SEM), operating with secondary electron mode at an accelerating voltage of 20 kV and in a high vacuum mode. The energy dispersive X-ray spectroscopy (EDS) measurements were done using an EDAX Apollo X detector mounted with the SEM microscope.

The EDS analyses were repeated in at least 10 different areas for each sample, each time the scan area was not smaller than 100 x 100 µm. The aim was to prevent the appearance of the signal from the carbon abrasive tape used to mount the samples in the recorded EDS spectra. The average depth of X-ray emission during the measurement is approx. 5 µm. The representative EDS spectra for each studied sample type were illustrated in Figures S35-S38.

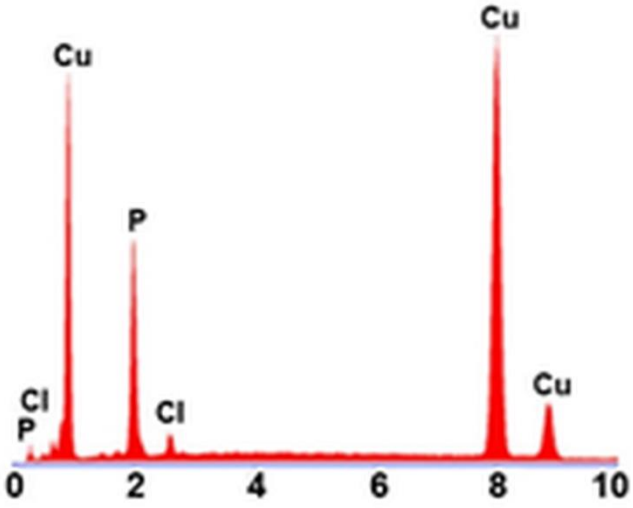

Figure S32. EDS spectrum for decomposed **Cu1** complex.

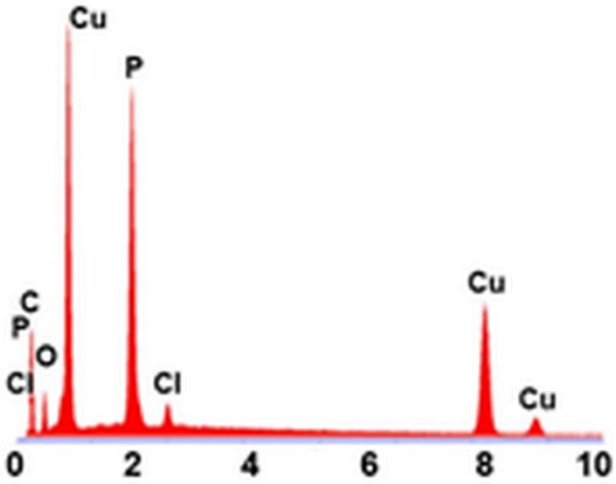

Figure S33. EDS spectrum for decomposed **Cu2** complex.

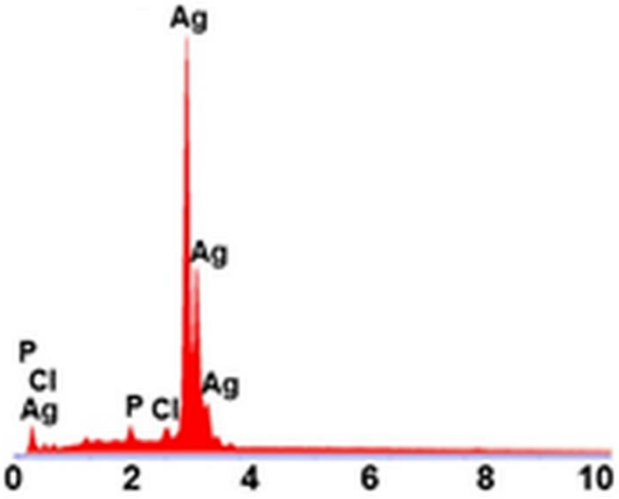

Figure S34. EDS spectrum for decomposed **Ag1** complex.

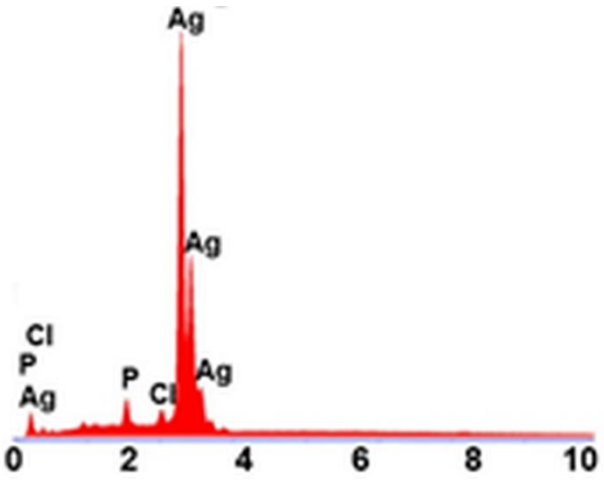

Figure S35. EDS spectrum for decomposed **Ag2** complex.

Table S4. The average chemical composition (in at.%) obtained on the basis of not less than ten EDS area analysis for each studied sample and M : P stoichiometries based on the EDS examinations (M = Cu or Ag respectively).

	Ag	Cu	P	Cl	O	C	M : P ratio
Cu1	-	57.5 ± 4.3	38.5 ± 2.5	2.4 ± 0.1	-	--	1.5 : 1
Cu2	-	10.0 ± 3.0	8.5 ± 2.1	1.2 ± 0.4	11.8 ± 1.4	68.5 ± 4.1	1.2 : 1
Ag1	89.4 ± 2.9	-	9.0 ± 2.1	1.6 ± 0.4	-	-	9.9 : 1
Ag2	61.2 ± 0.6	-	30.8 ± 1.3	8.0 ± 0.7	-	-	2.0 : 1

PART F. REFERENCES

1. Sheldrick, G. A short history of SHELX. *Acta Crystallogr. A* **2008,** 64 (1), 112-122.

2. Farrugia, L. WinGX and ORTEP for Windows: an update. *J. Appl. Cryst.* **2012,** 45 (4), 849-854.

3. Frisch, M. J.; Trucks, G. W.; Schlegel, H. B.; Scuseria, G. E.; Robb, M. A.; Cheeseman, J. R.; Scalmani, G.; Barone, V.; Petersson, G. A.; Nakatsuji, H.; Li, X.; Caricato, M.; Marenich, A. V.; Bloino, J.; Janesko, B. G.; Gomperts, R.; Mennucci, B.; Hratchian, H. P.; Ortiz, J. V.; Izmaylov, A. F.; Sonnenberg, J. L.; Williams; Ding, F.; Lipparini, F.; Egidi, F.; Goings, J.; Peng, B.; Petrone, A.; Henderson, T.; Ranasinghe, D.; Zakrzewski, V. G.; Gao, J.; Rega, N.; Zheng, G.; Liang, W.; Hada, M.; Ehara, M.; Toyota, K.; Fukuda, R.; Hasegawa, J.; Ishida, M.; Nakajima, T.; Honda, Y.; Kitao, O.; Nakai, H.; Vreven, T.; Throssell, K.; Montgomery Jr., J. A.; Peralta, J. E.; Ogliaro, F.; Bearpark, M. J.; Heyd, J. J.; Brothers, E. N.; Kudin, K. N.; Staroverov, V. N.; Keith, T. A.; Kobayashi, R.; Normand, J.; Raghavachari, K.; Rendell, A. P.; Burant, J. C.; Iyengar, S. S.; Tomasi, J.; Cossi, M.; Millam, J. M.; Klene, M.; Adamo, C.; Cammi, R.; Ochterski, J. W.; Martin, R. L.; Morokuma, K.; Farkas, O.; Foresman, J. B.; Fox, D. J. *Gaussian Rev. D.01*, Wallingford, CT, 2016.

4. Becke, A. D. Density-functional exchange-energy approximation with correct asymptotic behavior. *Phys. Rev. A* **1988,** 38 (6), 3098-3100.

5. Becke, A. D. Density-functional thermochemistry. III. The role of exact exchange. *J. Chem. Phys.* **1993,** 98 (7), 5648-5652.

6. Floch, P. L. Phosphaalkene, phospholyl and phosphinine ligands: New tools in coordination chemistry and catalysis. *Coord. Chem. Rev.* **2006,** 250 (5), 627-681.

7. Glendening, E. D.; Reed, A. E.; Carpenter, J. E.; Weinhold, F. NBO Version 3.1.

8. Chai, J.-D.; Head-Gordon, M. Long-range corrected hybrid density functionals with damped atom–atom dispersion corrections. *Phys. Chem. Chem. Phys.* **2008,** 10 (44), 6615-6620.

9. Grimme, S. Density functional theory with London dispersion corrections. *Wiley Interdiscip. Rev. Comput. Mol. Sci.* **2011,** 1 (2), 211-228.

10. Weigend, F. Accurate Coulomb-fitting basis sets for H to Rn. *Phys. Chem. Chem. Phys.* **2006,** 8 (9), 1057-1065.

11. Weigend, F.; Ahlrichs, R. Balanced basis sets of split valence, triple zeta valence and quadruple zeta valence quality for H to Rn: Design and assessment of accuracy. *Phys. Chem. Chem. Phys.* **2005,** 7 (18), 3297-3305.